https://doi.org/10.5194/bg-2021-20
Preprint. Discussion started: 30 March 2021

Biogeosciences Discussions Open Access EGU

Impact of dust addition on the metabolism of Mediterranean plankton communities and carbon export under present and future conditions of pH and temperature

Frédéric Gazeau[1], France Van Wambeke[2], Emilio Marañón[3], María Pérez-Lorenzo[3], Samir Alliouane[1], Christian Stolpe[1], Thierry Blasco[1], Nathalie Leblond[4], Birthe Zäncker[5,6], Anja Engel[6], Barbara Marie[7], Julie Dinasquet[7,8], Cécile Guieu[1]

[1] Sorbonne Université, CNRS, Laboratoire d'Océanographie de Villefranche, LOV, 06230 Villefranche-sur-Mer, France
[2] Aix-Marseille Université, Université de Toulon, CNRS/INSU, IRD, Mediterranean Institute of Oceanography (MIO), UM 110, 13288, Marseille, France
[3] Department of Ecology and Animal Biology, Universidade de Vigo, 36310 Vigo, Spain
[4] Sorbonne Université, CNRS, Institut de la Mer de Villefranche, IMEV, 06230 Villefranche-sur-Mer, France
[5] The Marine Biological Association of the UK, PL1 2PB Plymouth, United Kingdom
[6] GEOMAR Helmholtz Centre for Ocean Research, Kiel, Germany
[7] CNRS, Sorbonne Université, Laboratoire d'Océanographie Microbienne, LOMIC, F-66650 Banyuls-sur-Mer, France
[8] Scripps Institution of Oceanography, University of California San Diego, USA

Correspondence to: Frédéric Gazeau (f.gazeau@obs-vlfr.fr)

Keywords: Mediterranean Sea; Atmospheric deposition; Plankton community metabolism; Carbon export; Ocean acidification; Ocean warming

https://doi.org/10.5194/bg-2021-20
Preprint. Discussion started: 30 March 2021

Biogeosciences Discussions Open Access EGU

Abstract

Although atmospheric dust fluxes from arid as well as human-impacted areas represent a significant source of nutrients to surface waters of the Mediterranean Sea, studies focusing on the evolution of the metabolic balance of the plankton community following a dust deposition event are scarce and none were conducted in the context of projected future levels of temperature and pH. Moreover, most of the experiments took place in coastal areas. In the framework of the PEACETIME project, three dust-addition perturbation experiments were conducted in 300-L tanks filled with surface seawater collected in the Tyrrhenian Sea (TYR), Ionian Sea (ION) and in the Algerian basin (FAST) onboard the R/V "Pourquoi Pas?" in late spring 2017. For each experiment, six tanks were used to follow the evolution of chemical and biological stocks, biological activity and particle export. The impacts of a dust deposition event simulated at their surface were followed under present environmental conditions and under a realistic climate change scenario for 2100 (ca. + 3 °C and -0.3 pH units). The tested waters were all typical of stratified oligotrophic conditions encountered in the open Mediterranean Sea at this period of the year, with low rates of primary production and a metabolic balance towards net heterotrophy. The release of nutrients after dust seeding had very contrasting impacts on the metabolism of the communities, depending on the station investigated. At TYR, the release of new nutrients was followed by a negative impact on both particulate and dissolved ^{14}C-based production rates, while heterotrophic bacterial production strongly increased, driving the community to an even more heterotrophic state. At ION and FAST, the efficiency of organic matter export due to mineral/organic aggregation processes was lower than at TYR likely related to a lower quantity/age of dissolved organic matter present at the time of the seeding. At these stations, both

https://doi.org/10.5194/bg-2021-20
Preprint. Discussion started: 30 March 2021

the autotrophic and heterotrophic community benefited from dust addition, with a stronger relative increase in autotrophic processes observed at FAST. Our study showed that the potential positive impact of dust deposition on primary production depends on the initial composition and metabolic state of the investigated community. This potential is constrained by the quantity of nutrients added in order to sustain both the fast response of heterotrophic prokaryotes and the delayed one of primary producers. Finally, under future environmental conditions, heterotrophic metabolism was overall more impacted than primary production, with the consequence that all integrated net community production rates decreased with no detectable impact on carbon export, therefore reducing the capacity of surface waters to sequester anthropogenic CO_2.

https://doi.org/10.5194/bg-2021-20
Preprint. Discussion started: 30 March 2021

54

55 1. Introduction

56 Low Nutrient Low Chlorophyll (LNLC) areas represent 60% of the global ocean surface
57 area (Longhurst et al., 1995) and, although phytoplankton production there is limited by the
58 availability of nitrogen, phosphorus and iron, it accounts for 50% of global carbon export
59 (Emerson et al., 1997). Atmospheric dust fluxes from arid as well as anthropogenic sources
60 represent a significant source of these nutrients to surface waters in these regions and as such
61 could play a significant role in stimulating primary production (e.g. Bishop et al., 2002; Guieu et
62 al., 2014b; Jickells and Moore, 2015), potentially increasing the efficiency of the biological
63 pump in the sequestration of atmospheric CO_2. However, as heterotrophic prokaryotes have been
64 shown to outcompete phytoplankton during nutrient addition experiments (e.g. Guieu et al.,
65 2014a; Mills et al., 2008; Thingstad et al., 2005), dust deposition could induce even stronger
66 enhancements of heterotrophic bacterial production and/or respiration rates thereby reducing net
67 atmospheric CO_2 drawdown and the potential for carbon export outside the euphotic zone (Guieu
68 et al., 2014b). Indeed, several experiments conducted in the Atlantic Ocean and in the
69 Mediterranean Sea have shown a fast and dominant effect of dust additions on heterotrophic
70 bacterioplankton metabolism (Herut et al., 2005, 2016; Lekunberri et al., 2010; Marañón et al.,
71 2010; Pulido-Villena et al., 2008, 2014). However, to the best of our knowledge, no study
72 focused on the evolution of the metabolic balance of the plankton community after such a dust
73 event in the open sea. The metabolic balance (or net community production, NCP) is defined as
74 the difference between gross primary production (GPP) of autotrophic organisms and community

https://doi.org/10.5194/bg-2021-20
Preprint. Discussion started: 30 March 2021

75 respiration (CR) of both autotrophic and heterotrophic organisms, revealing the capacity of a
76 system to sequester carbon via the biological pump.

77 The Mediterranean Sea is a perfect example of LNLC regions and receives anthropogenic
78 aerosols originating from industrial and domestic activities from all around the basin and other
79 parts of Europe and pulses of natural inputs from the Sahara (e.g. Bergametti et al., 1989;
80 Desboeufs et al., 2018). These atmospheric depositions, mostly in the form of pulsed inputs
81 (Loÿe-Pilot and Martin, 1996), provide new nutrients (Guieu et al., 2010; Kouvarakis et al.,
82 2001; Markaki et al., 2003; Ridame and Guieu, 2002) to the surface waters with fluxes that are of
83 the same order of magnitude as riverine inputs (Powley et al., 2017). These significant nutrient
84 enrichments likely support primary production especially during the stratification period (Bonnet
85 et al., 2005; Ridame and Guieu, 2002), however no clear correlation between dust and ocean
86 color have been evidenced from long series of satellite observations (Guieu and Ridame, 2020).
87 This raises the question on which compartment (autotrophic or heterotrophic) benefits the most
88 from these transient relieves in nutrient limitation.

89 In response to ocean warming and increased stratification, LNLC areas are expected to
90 expand in the future (Irwin and Oliver, 2009; Polovina et al., 2008) due to lower nutrient supply
91 from sub-surface waters (Behrenfeld et al., 2006). Furthermore, dust deposition could increase in
92 the future due to desertification (Moulin and Chiapello, 2006), although so far the trend for
93 deposition remains uncertain because the drying of the Mediterranean basin might also induce
94 less wet deposition over the basin (Laurent et al., 2021). Nevertheless, whether the fluxes
95 increase or not in the coming decades and centuries, new nutrients from atmospheric sources will
96 play an important role in a surface mixed layer even more stratified and isolated from the deeper
97 nutrient-rich layer. The question remains on how plankton metabolism and carbon export would

https://doi.org/10.5194/bg-2021-20
Preprint. Discussion started: 30 March 2021

respond in a warmer and more acidified ocean. Indeed, with an average annual anthropogenic CO_2 uptake, during the period 2010 to 2019, of 2.5 ± 0.6 GtC (~22.9% of anthropogenic emissions; Friedlingstein et al., 2020), the oceans substantially contribute towards slowing down the increase in atmospheric CO_2 concentrations, and therefore towards limiting terrestrial and ocean warming. However, this massive CO_2 input induces global changes in seawater chemistry referred to as "ocean acidification" because increased CO_2 concentration lowers seawater pH (i.e. increases its acidity).

Although the response of plankton metabolism to ocean warming has been shown to be highly dependent on resource availability (Lewandowska et al., 2014), both for heterotrophic bacteria (Lopez-Urrutia and Moran, 2007) and phytoplankton (Marañón et al., 2018), it has been suggested that ocean warming will substantially weaken the ocean CO_2 sink in the future as a consequence of stronger increase in remineralization than in photosynthesis processes, following the metabolic theory of ecology (MTE; Brown et al., 2004; Gillooly et al., 2001). Ocean acidification alone has been shown to exert no or very limited influence on plankton metabolism in the Mediterranean Sea (Maugendre et al., 2017a; Mercado et al., 2014). To the best of our knowledge, only Maugendre et al. (2015) studied the combined impact of ocean warming and acidification on plankton metabolism in the Mediterranean Sea. They found a very limited impact of ocean acidification on the plankton community and a positive impact of warming on small phytoplankton species (e.g. Cyanobacteria) with a potential decrease of the export and energy transfer to higher trophic levels. Nevertheless, that study was conducted under nutrient depleted conditions and there is still a need to assess the combined impact of warming and acidification on the metabolic balance of plankton communities in this region, following a transient relief in nutrient availability (Maugendre et al., 2017b).

https://doi.org/10.5194/bg-2021-20
Preprint. Discussion started: 30 March 2021

So far there has been no attempt to evaluate the evolution of plankton metabolism and carbon export following atmospheric deposition in the context of future levels of temperature and pH. Such experiments were conducted in the frame of the PEACETIME project (ProcEss studies at the Air-sEa Interface after dust deposition in the MEditerranean sea; http://peacetime-project.org/) during the cruise on board the R/V "Pourquoi Pas?" in May/June 2017 (Guieu et al., 2020). The project aimed at extensively studying and parameterizing the chain of processes occurring in the Mediterranean Sea after atmospheric deposition, especially of Saharan dust, and to put them in perspective of on-going environmental changes. During this cruise, three perturbation experiments were conducted in 300-L tanks filled with surface seawater collected in the Tyrrhenian Sea (TYR), Ionian Sea (ION) and in the Algerian basin (FAST; Fig. 1). Six tanks were used to follow the evolution of chemical and biological stocks, biological activity and export, following a wet dust deposition event simulated at their surface, both under present environmental conditions and following a realistic climate change scenario for 2100 (ca. + 3 °C and -0.3 pH units; IPCC, 2013). A companion paper presents the general setup of the experiments and the impacts of dust under present and future environmental conditions on nutrients and biological stocks (Gazeau et al., 2020). Here, we focus on the impacts of dust seeding on plankton metabolism (e.g. primary production, heterotrophic prokaryote production) and carbon export.

https://doi.org/10.5194/bg-2021-20
Preprint. Discussion started: 30 March 2021

139

140 2. Material and Methods

141 2.1. General set-up

142 The general set-up of the experiments is fully detailed in Gazeau et al. (2020). Briefly,
143 three experiments were performed at the long duration stations TYR, ION and FAST during the
144 Peacetime cruise onboard R/V "Le Pourquoi Pas?" (Fig. 1). During these experiments (3 to 4
145 days each), seawater was incubated in 300-L tanks (Fig. S1) installed in a temperature-controlled
146 container, in which the irradiance spectrum and intensity can be finely controlled and in which
147 future ocean acidification and warming conditions can be fully reproduced. The tanks were made
148 of high-density polyethylene (HDPE) and were trace-metal free in order to avoid contaminations,
149 with a height of 1.09 m, a diameter of 0.68 m, a surface area of 0.36 m^2 and a volume of 0.28 m^3.
150 The conical base of the tanks was equipped with a sediment trap that was left open during the
151 duration of the experiments and removed at the end. The experimental protocol comprised two
152 unmodified control tanks (C1 and C2), two tanks enriched with Saharan dust (D1 and D2) and
153 two tanks enriched with Saharan dust and maintained simultaneously under warmer (+ 3 ºC) and
154 acidified (-0.3 pH unit) conditions (G1 and G2). At the three stations, tanks were always filled at
155 the end of the day before the start of the experiments: TYR (17/05/2017), ION (25/05/2017) and
156 FAST (02/06/2017). The tanks were filled by means of a large peristaltic pump (Verder© VF40
157 with EPDM hose, flow of 1200 L h^{-1}) collecting seawater below the base of the boat (depth of ~
158 5 m), used to supply continuously surface seawater to a series of instruments during the entire
159 campaign. While filling the tanks, seawater was sampled for the measurements of selected
160 parameters (sampling time = t-12h). After filling the tanks, seawater was slowly warmed

https://doi.org/10.5194/bg-2021-20
Preprint. Discussion started: 30 March 2021

overnight using 500 W heaters, controlled by temperature-regulation units (COREMA©), in G1 and G2 to reach an offset of + 3 °C. ^{13}C-bicarbonate was added to all tanks at 4:00 am (all times in local time) and G1 and G2 were acidified by addition of CO_2-saturated filtered (0.2 µm) seawater (~1.5 L in 300 L; collected when filling the tanks at each station) at 4:30 am to reach a pH offset of -0.3. Sampling for many parameters took place prior to dust seeding (sampling time = t0). Dust seeding was performed between 7:00 and 9:00 in tanks D1, D2, G1 and G2. The same dust analog was used and the same dust flux was simulated as for the DUNE 2009 experiments described in Desboeufs et al. (2014). To mimic a realistic wet flux event of 10 g m^{-2}, 3.6 g of this analog dust were quickly diluted into 2 L of ultrahigh-purity water (UHP water; 18.2 MΩ cm^{-1} resistivity), and sprayed at the surface of the tanks using an all-plastic garden sprayer (duration = 30 min). Depending on the considered parameter or process, seawater sampling was conducted 1 h (t1h), 6 h (t6h), 12 h (t12h), 24 h (t24h), 48 h (t48h) and 72 h (t72h) (+ 96 h = t96h for station FAST) after dust addition. Acid-washed silicone tubes were used for transferring the water collected from the tanks to the different vials or containers.

2.2. Stocks

2.2.1. Dissolved and particulate organic carbon

The concentration of dissolved organic carbon (DOC) was determined from duplicate 10 mL GF/F (pre-combusted , Whatman) filtered subsamples that were transferred to pre-combusted glass ampoules, acidified with H_3PO_4 (final pH = 2) and sealed. The sealed glass ampoules were stored in the dark at room temperature until analysis at the Laboratoire d'Océanographie Microbienne (LOMIC). DOC measurements were performed on a Shimadzu© TOC-V-CSH

https://doi.org/10.5194/bg-2021-20
Preprint. Discussion started: 30 March 2021

(Benner and Strom, 1993). Prior to injection, DOC samples were sparged with CO_2-free air for 6 min to remove inorganic carbon. Sample (100 µL) were injected in triplicate and the analytical precision was 2%. Standards were prepared with acetanilid.

Seawater samples for measurements of particulate organic carbon concentrations (POC; 2 L) were taken at t-12h, t0, t12h, t24h, t48h and t72h (or t96h for station FAST), filtered on pre-combusted GF/F membranes, dried at 60 °C and analyzed at the Laboratoire d'Océanographie de Villefranche (LOV, France) following decarbonatation with a drop of HCl 2N, on an elemental analyzer coupled with an isotope ratio mass spectrometer (EA-IRMS; Vario Pyrocube-Isoprime 100, Elementar©).

2.2.2. Total hydrolysable carbohydrates and amino acids

For total hydrolysable carbohydrates and amino acids, samples were taken at t0, t6h, t24h, t48h and t72h at all stations. For total hydrolysable carbohydrates (TCHO) > 1 kDa, samples (20 mL) were filled into pre-combusted glass vials (8 h, 500 °C) and stored at -20 °C pending analysis. Prior to analysis, samples were desalted with membrane dialysis (1 kDa MWCO, Spectra Por) at 1 °C for 5 h. Samples were subsequently hydrolyzed for 20 h at 100 °C with 0.8 M HCl final concentration followed by neutralization using acid evaporation (N_2, for 5 h at 50 °C). TCHO were analysed at GEOMAR using high performance anion exchange chromatography with pulsed amperometric detection (HPAEC-PAD), on a Dionex ICS 3000 ion chromatography system following the procedure of Engel and Händel (2011). Two replicates per TCHO sample were analyzed.

For total hydrolysable amino acids (TAA), samples (5 mL) were filled into pre-combusted glass vials (8 h, 500 °C) and stored at -20 °C. Samples were hydrolyzed at 100 °C for

https://doi.org/10.5194/bg-2021-20
Preprint. Discussion started: 30 March 2021

20 h with 1 mL 30% HCl (Suprapur®, Merck) added to 1 mL of sample, and neutralized by acid evaporation under vacuum at 60 °C in a microwave. Samples were analyzed by high performance liquid chromatography (HPLC) using an Agilent 1260 HPLC system following a modified version of established methods (Dittmar et al., 2009; Lindroth and Mopper, 1979). Separation of 13 amino acids with a C18 column (Phenomenex Kinetex, 2.6 µm, 150 x 4.6 mm) was obtained after in-line derivatization with o-phthaldialdehyde and mercaptoethanol. A gradient with solvent A containing 5 % acetonitrile (LiChrosolv, Merck, HPLC gradient grade) in sodium dihydrogenphosphate (Suprapur®, Merck) buffer (pH 7.0) and solvent B being acetonitrile was used for analysis. A gradient from 100% solvent A to 78% solvent A was produced in 50 min. Two replicates per TAA sample were analyzed.

2.2.3. Transparent exopolymer particles

Samples for transparent exopolymer particles (TEP) were taken at t0, t24h and t72h at all stations. The abundance and area of TEP were microscopically measured following the procedure given in Engel (2009). Samples of 10-50 mL were directly filtered under low vacuum (< 200 mbar) onto a 0.4 µm Nucleopore membrane (Whatman©) filter, stained with 1 mL Alcian Blue solution (0.2 g l^{-1} w/v) for 3 s and rinsed with MilliQ water. Filters were mounted on Cytoclear© slides and stored at -20 °C until analysis. Two filters per sample with 30 images each were analyzed using a Zeiss Axio Scope.A1 (Zeiss©) and an AxioCam MRc (Zeiss©). The pictures with a resolution of 1388 x 1040 pixels were saved using AxioVision LE64 Rel. 4.8 (Zeiss©). All particles larger than 0.2 µm^2 were analyzed. ImageJ© and R were subsequently used for image analysis (Schneider, Rasband and Eliceiri 2012, R Core Team, 2014). Filters prepared with 10 mL MilliQ water instead of samples served as a blank. The carbon content of TEP (TEP-C) was estimated after Mari (1999) using the size-dependent relationship:

https://doi.org/10.5194/bg-2021-20
Preprint. Discussion started: 30 March 2021

227 $TEP\text{-}C = a\ \Sigma_i\ n_i\ r_i^D$ (1)

228 with n_i being the number of TEP in the size class i and r_i being the mean equivalent spherical
229 radius of the size class. The constant $a = 0.25 * 10^{-6}$ (µg C) and the fractal dimension of
230 aggregates $D = 2.55$ were used as proposed by Mari (1999). To relate to organic carbon
231 concentration in seawater, data for TEP-C are given as µmol L^{-1}.

232 2.3. Processes

233 2.3.1. Dissolved and particulate ^{14}C incorporation rates

234 The photosynthetic production of particulate (< 0.2-2 µm and > 2 µm size fractions) and
235 dissolved organic matter was determined from samples taken at t0, t24h, t48h and t72h (or t96h
236 at station FAST) with the ^{14}C-uptake technique. From each tank, four polystyrene bottles (70
237 mL; three light and one dark bottles) were filled with sampled seawater and amended with 40
238 µCi of $NaH^{14}CO_3$. Bottles were incubated for 8 h in two extra 300 L tanks maintained under
239 similar light and temperature regimes than in the experimental tanks (ambient temperature for
240 C1, C2, D1 and D2 and ambient temperature + 3 °C for G1 and G2). Incubations were
241 terminated by sequential filtration of the sample through polycarbonate filters (pore sizes 2 µm
242 and 0.2 µm, 47 mm diameter) using low-pressure vacuum. Filters were exposed for 12 h to
243 concentrated HCl fumes to remove non-fixed, inorganic ^{14}C, and then transferred to 4 mL plastic
244 scintillation vials to which 3.5 mL of scintillation cocktail (Ultima Gold XR, Perkin Elmer©)
245 were added. For the measurement of dissolved primary production, a 5 mL aliquot of each
246 sampling bottle was filtered, at the end of incubation, through a 0.2 µm polycarbonate filter (25
247 mm diameter). This filtration was conducted, under low-pressure vacuum, in a circular filtration

https://doi.org/10.5194/bg-2021-20
Preprint. Discussion started: 30 March 2021

manifold that allows the recovery of the filtrate into 20 mL scintillation vials. The filtrates were acidified with 200 µL of 50% HCl and maintained in an orbital shaker for 12 h. Finally, 15 mL of liquid scintillation cocktail was added to each sample. All filter and filtrate samples were measured onboard in a liquid scintillation counter (Packard© 1600 TR). ^{14}C-based production rates (PP; in µg C L^{-1} h^{-1}) were calculated as:

$$PP = C_T \times \left(\frac{DPM_{sample} - DPM_{dark}}{DPM_{added} \times t} \right) \quad (2)$$

where C_T is the concentration of total dissolved inorganic carbon (µg C L^{-1}), DPM_{sample} and DPM_{dark} are the radioactivity counts in the light and dark bottle, respectively, DPM_{added} is the radioactivity added to each sample, and t is the incubation time (h).

The percentage extracellular release (PER%) was calculated as:

$$PER\% = \frac{PPd}{PPd + PPp} \times 100 \quad (3)$$

where PPd refers to ^{14}C-based dissolved production and PPp refers to ^{14}C-based particulate production (sum of < 2 and > 2 µm size fractions).

2.3.2. Integrated ^{13}C incorporation

Addition of ^{13}C-bicarbonate ($NaH^{13}CO_3$ 99%; Sigma-Aldrich©) was performed in each tank before t0 in order to increase the isotopic level (δ^{13}C signature) of the dissolved inorganic carbon pool to ca. 350‰. We followed with time the evolution of the δ^{13}C signature in dissolved inorganic carbon (δ^{13}C-C_T), dissolved organic carbon (δ^{13}C-DOC) and particulate organic carbon pools (δ^{13}C-POC). For the analysis of the actual δ^{13}C-C_T, 60 mL of sampled seawater (at t-12h, t0, t12h, t24h, t48h and t72h; + t96h at station FAST) was gently transferred to glass vials

https://doi.org/10.5194/bg-2021-20
Preprint. Discussion started: 30 March 2021

avoiding bubbles. Vials were sealed after being poisoned with 12 µL saturated $HgCl_2$ and stored upside-down at room temperature in the dark pending analysis. At the University of Leuven, a helium headspace (5 mL) was created in the vials and samples were acidified with 2 mL of phosphoric acid (H_3PO_4, 99%). Samples were left to equilibrate overnight to transfer all C_T to gaseous CO_2. Samples were injected in the carrier gas stream of an EA-IRMS (Thermo© EA1110 and Delta V Advantage), and data were calibrated with NBS-19 and LSVEC standards (Gillikin and Bouillon, 2007).

At the same frequency than for $\delta^{13}C$-C_T, samples for $\delta^{13}C$-DOC were filtered online (see above), transferred to 40 mL pre-cleaned borosilicate amber EPA vials with septa caps (PTFE-lined silicone) and stored in the dark pending analysis at the Ján Veizer Stable Isotope Laboratory (Ottawa, Canada).

At t-12h, t0, t12h, t24h, t48h and t72h (or t96h at station FAST), the $\delta^{13}C$-POC was obtained based on the same measurements as described above for POC, on a an elemental analyzer coupled with an isotope ratio mass spectrometer (EA-IRMS; Vario Pyrocube-Isoprime 100, Elementar©).

Carbon isotope data are expressed in the delta notation (δ) relative to Vienna Pee Dee Belemnite (VPDB) standard. The carbon isotope ratio was calculated as:

$$R_{sample} = \left(\frac{\delta^{13}C_{sample}}{1000} + 1\right) \text{x } R_{VPDB} \quad (4)$$

with $R_{VPDB} = 0.011237$.

https://doi.org/10.5194/bg-2021-20
Preprint. Discussion started: 30 March 2021

2.3.2. Community metabolism (oxygen light-dark method)

At the same frequency as for ^{14}C incorporation, from each tank, a volume of 2 L was sampled in plastic bottles and distributed in 15 biological oxygen demand (BOD; 60 mL) borosilicate bottles. Five BOD bottles were immediately fixed with Winkler reagents (initial O_2 concentrations), five BOD bottles were incubated in the dark for the measurement of community respiration (CR) in two incubators maintained respectively at ambient temperature for C1, C2, D1 and D2 and at ambient temperature + 3 °C for G1 and G2. Additionally, five BOD bottles were incubated for the measurement of net community production (NCP) in the same tanks as described above for ^{14}C-incorporation. Upon completion of the incubations (24 h), samples were fixed with Winkler reagents. Within one day, O_2 concentrations were measured using an automated Winkler titration technique with potentiometric endpoint detection. Analyses were performed on board with a Metrohm© Titrando 888 and a redox electrode (Metrohm© Au electrode). Reagents and standardizations were similar to those described by Knap et al. (1996). NCP and CR were estimated by regressing O_2 values against time, and CR was expressed as negative values. Gross primary production (GPP) was calculated as the difference between NCP and CR. The combined standard errors were calculated as:

$$SE_{xy} = \sqrt{SE_x^2 + SE_y^2} \quad (5)$$

https://doi.org/10.5194/bg-2021-20
Preprint. Discussion started: 30 March 2021


Biogeosciences Discussions Open Access EGU

304 ## 2.3.4. Heterotrophic prokaryotic production and

305 ## ectoenzymatic activities

306 At all sampling times, heterotrophic bacterial production (BP, *sensus stricto* referring
307 to heterotrophic prokaryotic production) was determined onboard using the microcentrifuge
308 method with the ^{3}H- leucine (^{3}H-Leu) incorporation technique to measure protein production
309 (Smith and Azam, 1992). The detailed protocol is in Van Wambeke et al. (2020b). Briefly,
310 triplicate 1.5 mL samples and one blank were incubated in the dark for 1-2 h in two
311 thermostated incubators maintained respectively at ambient temperature for C1, C2, D1 and
312 D2 and at ambient temperature +3 °C for G1 and G2. Incubations were ended by the addition
313 of TCA to a final concentration of 5%, followed by three runs of centrifugation at 16000 g
314 for 10 min. Pellets were rinsed with TCA 5% and ethanol 80%. A factor of 1.5 kg C mol
315 leucine^{-1} was used to convert the incorporation of leucine to carbon equivalents, assuming no
316 isotopic dilution (Kirchman et al., 1993).

317 Ectoenzymatic activities were measured fluorometrically, using fluorogenic model
318 substrates that were L-leucine-7-amido-4-methyl-coumarin (Leu-MCA) and 4
319 methylumbelliferyl – phosphate (MUF-P) to track aminopeptidase activity (LAP) and
320 alkaline phosphatase activity (AP), respectively (Hoppe, 1983). Stocks solutions (5mM)
321 were prepared in methycellosolve and stored at -20 °C. Release of the products of LAP and
322 AP activities, MCA and MUF, were followed by measuring increase of fluorescence (exc/em
323 380/440 nm for MCA and 365/450 nm for MUF, wavelength width 5 nm) in a
324 VARIOSCAN LUXmicroplate reader calibrated with standards of MCA and MUF solutions.
325 For measurements, 2 mL of unfiltered samples from the tanks were supplemented with 100

https://doi.org/10.5194/bg-2021-20
Preprint. Discussion started: 30 March 2021

µL of a fluorogenic substrate solution diluted so that different concentrations were dispatched in a black 24-well polystyrene plate in duplicate (0.025, 0.05, 0.1, 0.25, 0.5, 1 µM for MUF-P, 0.5, 1, 5, 10, 25 µM for MCA-leu). Incubations were carried out in the same thermostatically controlled incubators than those used for BP and reproducing temperature levels in the experimental tanks. Incubations lasted up to 12 h long with a reading of fluorescence every 1 to 2 h, depending on the intended activities. The rate was calculated from the linear part of the fluorescence versus time relationship. Boiled-water blanks were run to check for abiotic activity. From varying velocities obtained, we determined the parameters Vm (maximum hydrolysis velocity) and Km (Michaelis-Menten constant which reflects enzyme affinity for the substrate) by fitting the data using a non-linear regression on the following equation:

$$V = V_m \, x \frac{S}{K_m + S} \quad (6)$$

where V is the hydrolysis rate and S the fluorogenic substrate concentration added.

2.3.5. Inorganic and organic material export

At the end of each experiment (t72h for TYR and ION and t96 h for FAST, after artificial dust seeding), the sediment traps were removed, closed and stored with formaldehyde 4%. Back in the laboratory, after the swimmers were removed, the samples were rinsed to remove the salts and then freeze-dried. The total amount of material collected was first weighted to measure the total exported flux. Several aliquots were then weighted to measure the following components: total carbon and organic carbon, lithogenic and biogenic silicates and calcium. Total carbon was measured on an elemental analyzer coupled with an isotope ratio mass spectrometer (EA-IRMS;

https://doi.org/10.5194/bg-2021-20
Preprint. Discussion started: 30 March 2021

Vario Pyrocube-Isoprime 100, Elementar©). Particulate organic carbon (POC) was measured in the same way after removing inorganic carbon by acidification with HCl 2N. Particulate inorganic carbon (PIC) was obtained by subtracting particulate organic carbon from particulate total carbon. Calcium concentrations were measured by ICP-OES (Inductively Coupled Plasma - Optic Emission Spectrometry; Perkin-Elmer© Optima 8000) on acid digested samples (the organic matrix was removed by HNO_3 while the mineral aluminosilicate matrix was eliminated with HF). Biogenic silica (BSi) and Lithogenic silica (LSi) were measured by colorimetry (Analytikjena© Specor 250 plus spectrophotometer) after a NaOH/HF digestion, respectively (Mosseri et al., 2005). The carbonate fraction of the exported material was determined from particulate calcium concentrations ($\%CaCO_3 = 5/2$ x (%Ca). The organic matter fraction was calculated as 2 x (%POC). The lithogenic fraction was calculated as [total mass – (organic matter + $CaCO_3$ + opal) and was very comparable to the lithogenic fraction calculated from LSi (taking Si concentration in dust analog used for seeding from Desboeufs et al., 2014; ca. 11.9%). In the controls, the amount of material exported was low and the entire content of the traps was filtered in order to measure total mass and organic matter mass fluxes.

2.4. Data processing

All metabolic rates were integrated over the duration of the experiments using trapezoidal integrations and the relative changes (in %) in tanks D and G as compared to the controls (average between C1 and C2) were computed following:

$$\text{Relative change} = \left(\frac{\text{Rate}_{\text{Treatment}} - \text{Rate}_{\text{Controls}}}{\text{Rate}_{\text{Controls}}}\right) \text{ x } 100 \quad (7)$$

Where $\text{Rate}_{\text{Treatment}}$ is the integrated rate measured in treatments D and G (D1, D2, G1 or G2) and $\text{Rate}_{\text{Controls}}$ is the averaged integrated rates between the duplicate controls (treatment C). Daily

https://doi.org/10.5194/bg-2021-20
Preprint. Discussion started: 30 March 2021

370 rates of ^{14}C-based production were computed from hourly rates assuming a 14 h daylight period.
371 As incubations performed from samples taken at t0 (before dust addition) do not represent what
372 happened in the tanks between t0 and t24h, as a first assumption, we considered a linear
373 evolution between these rates and those measured from samples at t24h, and recomputed an
374 average value for the time interval t0 - t24 h. At FAST, no incubations were performed for ^{14}C
375 incorporation and oxygen metabolism between t72h and t96h, again an average rate between
376 rates measured from samples taken at t48h and t96h was used for this time interval. Since
377 bacterial respiration rates were not measured, bacterial growth efficiency (BGE, expressed as a
378 percentage) was estimated based on BP (carbon units) and community respiration (CR, oxygen
379 units). As BP was determined more often than CR during the first 48 h, hourly BP rates were
380 integrated using trapezoidal integrations during the time period when CR was measured. We
381 assumed that heterotrophic prokaryotes were responsible for 70% of CR (BR/CR ratio; Lemée et
382 al., 2002) and used a respiratory quotient (RQ) of 0.8 (del Giorgio and Williams, 2005),
383 following the equation:

384 $$BGE = \left(\frac{BP}{CR \times \frac{BR}{CR}\text{ratio} \times RQ + BP}\right) \times 100 \quad (8)$$

385 When BP varied following an exponential growth, we calculated growth rates (μ_{BP}) from linear
386 least square regression of ln BP rates versus time.

https://doi.org/10.5194/bg-2021-20
Preprint. Discussion started: 30 March 2021

3. Results

3.1. Initial conditions

Initial conditions in terms of the chemical and biological standing stocks measured while filling the tanks at the three stations are fully described in Gazeau et al. (2020). Briefly, the three experiments were conducted with surface seawater collected during stratified oligotrophic conditions typical of the open Mediterranean Sea at this period of the year (Table 1). Nitrate + nitrite (NO_x) concentrations were maximal at station FAST with a NO_x to dissolved inorganic phosphate (DIP) molar ratio of ~ 4.6. Very low NO_x concentrations were observed at stations TYR and ION (14 and 18 nmol L^{-1}, respectively). DIP concentrations were the highest at station TYR (17 nmol L^{-1}) and the lowest at the most eastern station (ION, 7 nmol L^{-1}). Consequently, the lowest NO_x:DIP ratio was measured at TYR (0.8), compared to ION and FAST (2.8 and 4.6, respectively). Silicate ($Si(OH_4)$) concentrations were similar at TYR and ION (~1 µmol L^{-1}) and the lowest at FAST (~0.6 µmol L^{-1}). Both POC and DOC concentrations were the highest at station TYR (12.9 and 72.2 µmol L^{-1}, respectively) and the lowest at FAST (6.0 and 69.6 µmol L^{-1}, respectively). Very low and similar concentrations of chlorophyll *a* were measured at the three stations (0.063 - 0.072 µg L^{-1}). Phytoplankton communities at stations TYR and ION were dominated by Prymnesiophytes followed by Cyanobacteria, while, at station FAST, the phytoplanktonic community was clearly dominated by photosynthetic prokaryotes. At all three stations, the proportion of pigments representative of larger species was very small (< 5%; Gazeau et al., 2020). Heterotrophic prokaryotes were the most abundant at station FAST (6.15 x 10^5 cells mL^{-1}) and the least abundant at station ION (2.14 x 10^5 cells mL^{-1}).

https://doi.org/10.5194/bg-2021-20
Preprint. Discussion started: 30 March 2021

Relatively similar ^{14}C-based particulate production rates were measured at the start of the experiments (t0) in the control tanks (C1 and C2) at station ION and FAST (ca. 0.014 - 0.015 µg C L^{-1} h^{-1}). At both stations, ca. 80% of the production was attributed to larger (> 2 µm) cells and the percentage of extracellular release (%PER) did not exceed 45%. Lower rates were estimated at station TYR (total particulate production of 0.08 µg C L^{-1} h^{-1}) from which 87.5% was due to large cells > 2 µm. A larger amount of ^{14}C incorporation was released as dissolved organic matter at station TYR compared to the two other stations (PER ca. 60%). Metabolic balance derived from oxygen measurements showed that, at all three stations, the community was net heterotrophic with a higher degree of heterotrophy at station TYR (NCP were -1.9, -0.2, -0.8 µmol O_2 L^{-1} d^{-1} at TYR, ION and FAST, respectively, as measured in the controls from seawater sampled at t0). CR and GPP rates were respectively the highest and the lowest at station TYR compared to the other two stations. Finally, BP rates were the highest at station FAST (35.8 ng C L^{-1} h^{-1}), intermediate at ION (26.1 ng C L^{-1} h^{-1}) and the lowest at TYR (21.3 ng C L^{-1} h^{-1}).

3.2. Changes in biological stocks

DOC concentrations showed a general increasing trend during the three experiments and a large variability between duplicates (Fig. 2). This variability appeared as soon as 1 h after dust seeding (t1h) while the range of variation at t0 (before dust seeding) was rather moderate (difference between minimal and maximal values in all tanks of 1.3, 6.2 and 4.3 µmol C L^{-1} at station TYR, ION and FAST, respectively). As a consequence of this variability, no clear impact of dust seeding (D) could be highlighted at station TYR and FAST. Indeed, DOC concentrations in the two duplicates (D1 and D2) were higher than values in the controls (C1 and C2) in only 33% of the samples along the experiments (after dust seeding). In contrast, at station ION, DOC concentrations appeared impacted by dust seeding as higher concentrations were almost

https://doi.org/10.5194/bg-2021-20
Preprint. Discussion started: 30 March 2021

431 systematically (83% of the time after dust seeding) measured for this treatment as compared to
432 control tanks at the same time. At all stations, this impact was somewhat exacerbated under
433 conditions of temperature and pH projected for 2100 (G1 and G2) as DOC concentrations were
434 almost all the time higher in these tanks than in control tanks (83 - 100% of the samples after
435 dust seeding, depending on the station).

436 Total hydrolysable carbohydrates and amino acids concentrations along the three
437 experiments are shown in Fig. S2. TCHO concentrations were quite variable between tanks
438 before dust seeding (t0; 649 - 954, 569 - 660 and 600 - 744 nmol L^{-1} at station TYR, ION and
439 FAST, respectively) and no visible impact of the treatments were visible at station TYR (TCHO
440 tended to decrease everywhere). In contrast, at station ION and FAST, values in dust amended
441 tanks increased and appeared higher than in control tanks towards the end of the experiments
442 although the large variability between duplicates tended to mask this potential effect. An impact
443 of dust seeding was much clearer for TAA concentrations that showed larger increases
444 throughout the three experiments in tanks D1 and D2 as compared to control tanks, this effect
445 being exacerbated for warmer and acidified tanks (G1 and G2). The ratio between TAA and
446 DOC concentrations (Fig. 2) showed increasing trends in tanks D and G during all three
447 experiments with a clear distinction between treatments at the end of the experiments (G > D >
448 C). The strongest increase was observed at station FAST in tanks G where final values were
449 above 3%.

450 Particulate organic carbon (POC) concentrations strongly decreased at all stations
451 between t-12h and t0, this decrease being the largest at station TYR where concentrations
452 dropped from 25.7 to 9.6 - 13.2 µmol C L^{-1} (Fig. 3). After dust seeding, POC concentrations did
453 not show clear temporal trends for the three experiments although a slight general increase could

https://doi.org/10.5194/bg-2021-20
Preprint. Discussion started: 30 March 2021

be observed at station FAST. Furthermore, no impact of dust seeding and warming/acidification could be observed for this parameter. While concentrations of transparent exopolymer particles (TEP-C) were rather constant through time in control tanks at the three stations, a large increase was observed in dust-amended tanks (D and G) with TEP-C reaching values up to ~2 µmol C L^{-1} in tank G1 at station TYR after 24 h (i.e. ~17% of POC concentration, Fig. 3). In all cases except for tank G2 at station ION, TEP-C further decreased towards the end of the experiments although concentrations remained well above those observed in the controls. As the variability between duplicated tanks G was rather high, no impact of warming/acidification on TEP dynamics could be highlighted at the three stations.

3.3. Changes in metabolic rates

^{14}C-based particulate production rates as measured during the different time intervals at the three stations were low in control tanks (maximal total particulate production of 0.34 µg L^{-1} h^{-1} at station FAST) and did not show any particular temporal dynamics (Fig. 4). In these tanks, the vast majority of particulate production was attributed to cells above 2 µm (65 - 89%). The percentage of extracellular release (%PER) was overall maximal at station TYR and minimal at station FAST with a tendency to decrease with time at the three stations although large variations were observed between duplicates.

Dust addition alone did not have any clear positive impact on all ^{14}C-based rates at station TYR, with even an observable decrease in production rates from larger cells (> 2 µm) compared to the controls. In contrast, at this station, dust seeding under warmer and acidified conditions (tanks G) had a positive effect on particulate production rates, this effect being particularly visible for cells < 2 µm and to a lesser extent on dissolved production with a general

https://doi.org/10.5194/bg-2021-20
Preprint. Discussion started: 30 March 2021

476 decrease of %PER. An important discrepancy between the duplicates of treatment G was
477 observable at the end of the experiment with much larger rates measured in tank G2.
478 In contrast to station TYR, an enhancement effect of dust addition was clearly visible at
479 station ION where all rates increased towards the end of this experiment reaching a maximal
480 total particulate production of 0.6 - 0.7 µg L^{-1} h^{-1} in tanks D1 and D2. Since this positive effect
481 was similar between small and larger cells, dust addition alone had no effect on the partitioning
482 of production at this station, with cells > 2 µm representing ~80% of total production. Although
483 being also positively impacted and increasing with time, dissolved production appeared less
484 sensitive than particulate production leading to an overall decrease of %PER at this station
485 following dust addition. These positive impacts of dust seeding on ^{14}C-based particulate
486 production rates were even more visible at this station under warmer and acidified conditions
487 (tanks G) with maximal rates more than doubled compared to those measured under present
488 conditions of temperature and pH (1.5 - 1.6 µg L^{-1} h^{-1}). Dust seeding under warmer and acidified
489 conditions had a slight impact on the partitioning of particulate production at this station with
490 smaller cells benefiting the most from these conditions. %PER remained between 20 and 30%.
491 At station FAST, similarly to station ION, total particulate production rates were clearly
492 enhanced by dust addition (tanks D) reaching maximal values during the incubation time interval
493 t48 - 56h. No clear increase was observed for total particulate production on the next incubation
494 (t96 - 120h) while production rates of cells larger than 2 µm increased and rates of smaller cells
495 decreased. However at FAST, in contrast to station ION, there was much less impact of
496 warming/acidification on all measured rates although rates measured on smaller cells (< 2 µm)
497 did not decrease at the end of the experiment as observed under present environmental

https://doi.org/10.5194/bg-2021-20
Preprint. Discussion started: 30 March 2021

conditions. %PER under both present conditions of temperature and pH (tanks D) decreased during this experiment reaching values lower than in the controls and in tanks G.

The initial enrichment of the tanks in ^{13}C-bicarbonate led to an increase in the ^{13}C signature of dissolved inorganic carbon (δ^{13}C-C_T) of above 300‰, with generally lower values measured in warmer and acidified tanks (G; Fig. S3). After this initial enrichment, δ^{13}C-C_T levels decreased linearly in all tanks. At stations TYR and ION, the isotopic signature of dissolved organic carbon (δ^{13}C-DOC; Fig. S3) increased with time, although these increases were rather low and limited to ~ 4‰ over the course of the experiments. In contrast to station TYR, at ION, an enhanced incorporation of ^{13}C into DOC was visible after 24 h in tanks D and G in comparison to control tanks. A similar observation was done at station FAST, especially at the end of the experiment, although much more variability was observed at this station.

The incorporation of ^{13}C onto particulate organic carbon (δ^{13}C-POC) is shown in Fig. 5. At all stations, δ^{13}C-POC increased with time but reached lower enrichment levels at station TYR as compared to ION and FAST. At this station, incorporation rates appeared smaller in dust-amended tanks under present environmental conditions (tanks D). As for ^{14}C-based production rates, an important discrepancy was observed between duplicates under future conditions of temperature and pH (tanks G) with much higher final δ^{13}C-POC at the end of the experiment in tank G2. At station ION, enrichment levels obtained at the end of the experiment were more important in dust-amended tanks reaching maximal levels of 73‰ in tank G2 at t72h. This enhancement effect was even more visible at station FAST with maximal enrichment levels of 146‰ (tank D2 at t96h). Since no sampling occurred at t72h, these enrichment levels cannot be directly compared to what was measured at station TYR and ION. However, by interpolating

https://doi.org/10.5194/bg-2021-20
Preprint. Discussion started: 30 March 2021

values at t72h assuming a linear increase between these time intervals, enrichment levels appeared similar although slightly higher for tanks D between station ION and FAST.

NCP rates as measured using the O_2 light-dark method showed that, under control conditions, the communities remained the vast majority of the time throughout the three experiments in a net heterotrophic state (NCP < 0; Fig. 6). This was especially true at station TYR where the lowest NCP rates were measured. At this station, dust addition whether under present or future conditions of temperature and pH did not switch the community towards net autotrophy but even drove the community towards a stronger heterotrophy. This was related to the fact that while gross primary production rates were not positively impacted, community respiration increased in tanks D and G. At station ION, dust addition alone (tanks D) led to a switch from net heterotrophy to net autotrophy after two days of incubation due to a stronger positive effect of dust on GPP than on CR. Under future environmental conditions (tanks G), the same observation was made with higher NCP and GPP rates than in tanks D. CR rates reacted quickly to these forcing factors in tanks G and initially (first incubation) drove the community towards a much stronger heterotrophy as compared to the other tanks. Finally, at station FAST, similarly to what was observed at ION, the community became autotrophic after two days of incubation in dust amended tanks as, although both GPP and CR were positively impacted by dust addition, this impact was less important for CR. Warming and acidification had a limiting impact on this enhancement, with a lower final NCP in tanks G compared to tanks D, a difference that can be related to an absence of effects of these environmental stressors on GPP while CR clearly increased at higher temperature and lower pH.

While BP remained constant or gradually increased in control tanks depending on the station, a clear and quick fertilization effect was observable following dust addition (treatment D

https://doi.org/10.5194/bg-2021-20
Preprint. Discussion started: 30 March 2021

543 and G) at all stations (Fig. 7). At station TYR, BP rates sharply increased to reach maximal
544 values at t24h, with an even stronger increase observed under warmer and acidified conditions
545 (tanks G). After this initial increase, rates slightly decreased towards the end of the experiment.
546 This fertilization effect appeared less important at station ION where lower maximal rates were
547 obtained after 24 h as compared to station TYR. Nevertheless, the same observations can be
548 made, namely, 1) higher rates were measured under future temperature and pH levels and 2) after
549 this initial sharp increase, rates gradually decreased towards the end of the experiment especially
550 in tanks G. At station FAST, a much stronger effect of warming/acidification was observed with
551 an important increase of BP in tanks G until 24 or 48 h post-seeding, depending on the duplicate.
552 A sharp decline was observed for this treatment until the end of the experiment although rates
553 remained higher than those measured in tanks C and D. The impact of dust addition under
554 present environmental conditions (tanks D) was somehow more limited than at the other stations
555 with a gradual increase until t72h with maximal rates ~ 40 - 100% higher than rates measured in
556 the controls. However, BP increased exponentially between t0 and t12h in all tanks including
557 controls, and in all experiments (Table 2). The growth rate of BP (μ_{BP}) in control tanks was the
558 highest at TYR, intermediate at ION and the lowest at FAST. μ_{BP} increased significantly in all
559 dust amended tanks compared to controls. Under future environmental scenarios, μ_{BP} tended to
560 increase compared to treatment D but with a variable relative change.
561 BGE increased in dust amended tanks under present environmental conditions (treatment
562 D) at TYR and ION, while no changes were detectable at station FAST due to a strong
563 discrepancy between control duplicates and overall higher BGE at this station in the controls
564 (Table 3). In contrast, warming and acidification exerted the strongest effect at station FAST
565 with a doubling of BGE between treatment G and D. Although an increase in BGE was also

https://doi.org/10.5194/bg-2021-20
Preprint. Discussion started: 30 March 2021

observed at the two other stations in treatment G as compared to present environmental conditions (treatment D), this increase was more limited (ca. 1 to 1.4-fold increase).

The alkaline phosphatase Vm (AP Vm) increased in all experiments after dust seeding, with amplified effects in G treatments (Fig. S4). Note that AP Vm increased also in the controls at TYR and FAST. In contrast, leucine aminopeptidase Vm (LAP vm) showed succession of peaks instead of continuously increasing (Fig. S4). It was higher in dust alone treatment (D) as compared to the controls at TYR and FAST. A larger variability between duplicates at ION prevents such an observation. At all stations, maximum velocities were measured under future environmental conditions (G). Vm being possibly influenced by enzyme synthesis but also by the number of cells inducing such enzymes, we computed also specific AP Vm per heterotrophic bacterial cell (Fig. 7). Specific AP Vm slightly increased during all experiments in controls and dust-amended tanks (D) with no visible differences between these treatments, a clear over-expression of this enzyme was observed under warmer and more acidified conditions (treatment G) especially at station FAST where velocities were enhanced by a ~8-fold at t96h.

3.4. Inorganic and organic material export

Both total mass and organic matter fluxes, as measured from analyses of the sediment traps at the end of each experiment, were extremely low under control conditions (Fig. 8). Additions of dust in tanks D and G led to a strong increase in both fluxes with a large variability between the duplicates of treatment D at ION. No clear changes between tanks maintained under present and future conditions of temperature and pH could be highlighted.

https://doi.org/10.5194/bg-2021-20
Preprint. Discussion started: 30 March 2021

4. Discussion

4.1. Initial conditions of the tested waters and evolution in controls

As discussed in the companion paper from Gazeau et al. (2020), the three sampling stations were typical of stratified oligotrophic conditions encountered in the open Mediterranean Sea in late spring / early summer. DOC concentrations at the start of the experiments were in the same range (60 - 75 µmol C L^{-1}) as those measured from samples collected in surface waters using clean sampling procedures (Van Wambeke et al., 2020b), revealing no contamination issues from our sampling device. TAA concentrations as measured in the tanks at t0 were also consistent with measurements from surface water samples (Van Wambeke et al., 2020b) with an average across stations and treatments of 254 ± 36 nmol L^{-1} (Fig. S2). In contrast, TCHO appeared higher at t0 (average across stations and treatments of 681 ± 98 nmol L^{-1}) than concentrations based on clean *in situ* sampling (average of 595 ± 43 nmol L^{-1}; Van Wambeke et al., 2020b). The decrease in POC concentrations between pumping (t-12h) and t0 for the three experiments, especially at station TYR (likely linked to higher initial concentrations), was likely a consequence of sedimentation of senescent cells and/or fecal pellets in our experimental systems, which are designed to evaluate the export of matter thanks to their conical shape. TEP concentrations were not quantified at t-12h and therefore there is no possibility to evaluate if sedimentation of these particles occurred before t0 in our tanks. At t0, larger and more abundant TEP were measured at station TYR compared to the two other stations (data not shown) leading to a larger contribution of TEP carbon content (TEP-C) to POC concentrations (Fig. 3).

https://doi.org/10.5194/bg-2021-20
Preprint. Discussion started: 30 March 2021

As a consequence of a very low availability in inorganic nutrients, TChl*a* and ^{14}C-based production rates were very low, all typical of oligotrophic conditions. Nano- and micro-phytoplanktonic cells (> 2 µm) contributed most of the ^{14}C-based particulate production (~ 80%), as found also on several on-deck incubations at the three stations (on average 73 ± 6%; Marañón et al., 2020). %PER values were also very similar to those measured during these on-deck incubations (~ 40-45%; see Marañón et al., 2020). This suggests no significant impact of our experimental protocol on rates and partitioning of ^{14}C-based production rates (i.e. sampling from the continuous seawater supply, delay of 12 h before initial measurements, artificial light etc.). The low values of chlorophyll stocks as well as of ^{14}C-based production rates are consistent with previous estimates based on direct measurements, satellite observations and modelling approaches in the same areas in late spring / early summer (e.g. Bosc et al., 2004; Lazzari et al., 2016; Moutin and Raimbault, 2002).

The metabolic balance was in favor of net heterotrophy at all stations at the start of the experiments (NCP < 0). Net heterotrophy in the open Mediterranean sea at this period of the year has been reported by Regaudie-de-Gioux et al. (2009) and Christaki et al. (2011) in agreement with our measurements at t0 in control tanks (Table 1). The lowest NCP and the highest CR rates were measured at station TYR, suggesting that the autotrophic plankton community was not very active at this station. This was confirmed by the ^{14}C-based particulate production rates, which were about half the ones measured at the other two stations. The community at TYR was most likely relying on regenerated nutrients, as shown by the highest levels of ammonium (NH_4^+) measured at the start of this experiment (Gazeau et al., 2020). As discussed in Guieu et al. (2020), a dust deposition event took place several days before the arrival of the vessel in this area, likely on May 10-12. This dust event was confirmed by inventory of particulate aluminium

https://doi.org/10.5194/bg-2021-20
Preprint. Discussion started: 30 March 2021

630 in the water column at several stations of the Tyrrhenian Sea including TYR, 6 to 9 d after the
631 event (Matthieu Bressac, pers. comm.). This dust deposition likely stimulated phytoplankton
632 growth and POC accumulation shortly after the deposition and consequently increased the
633 abundance of herbivorous grazers (copepods) and attracted carnivorous species (Feliú et al.,
634 2020), subsequently driving the community towards a net heterotrophic state that characterized
635 the initial condition of the experiment at this station. The optimal conditions for BP growth at
636 this station were also confirmed by the highest μ_{BP} growth rates obtained among the three
637 experiments (Table 2; 0.06 - 0.07 h^{-1}) in controls tanks.
638 The two other stations, although both also showing a slight net heterotrophic state, were
639 clearly different from each other in terms of initial biological stocks and metabolic rates. Indeed,
640 whereas TChl*a* and abundances of pico- and nano-autotrophic cells (flow cytometry counts;
641 Gazeau et al., 2020) were higher at FAST compared to ION, the autotrophic community was not
642 more efficient at fixing carbon at this station, as shown by similar initial ^{14}C-based production
643 rates. In contrast, both heterotrophic prokaryotic abundances and BP were much higher at station
644 FAST as compared to ION, leading to initial higher CR and lower NCP. At ION, the initial NCP
645 closer to metabolic balance further suggests a tight coupling between heterotrophic prokaryotes
646 and phytoplankton at this station, as discussed by Dinasquet et al. (2021).
647 For most of the chemical and biological stocks (e.g. nutrients, pigments etc.) presented in
648 Gazeau et al. (2020), no major changes took place during the three experiments under control
649 conditions. Here, we further show that DOC, POC as well as TEP concentrations did not exhibit
650 strong changes during the experiments. For DOC, large variability between the duplicates (C1
651 and C2) potentially masked an increase towards the end of the experiments. The same holds true
652 for autotrophic metabolic rates, as ^{14}C-based particulate production rates showed no marked

https://doi.org/10.5194/bg-2021-20
Preprint. Discussion started: 30 March 2021

variations during the three experiments, although a slight increase was visible at FAST until t48h. The communities at the three stations remained heterotrophic under the nutrient-limited conditions in the controls. However, heterotrophic prokaryotes probably benefited from initial inputs of available organic matter issued from other stressed eukaryotic organisms and/or POC decay between t-12h and t0, which could be due to both sedimentation and degradation. This was reflected in the progressive increase of BP, their variable initial growth rates (μ_{BP} ranged from 0.02 to 0.06 h^{-1} in control tanks according to the experiment) as well as increasing TAA/DOC ratios at the three stations. Finally, an initial increase of BP during incubations is generally described and classically attributed to a bottle effect, which favours large, fast-growing bacteria and often induces mortality of some phytoplankton cells (Calvo-Díaz et al., 2011; Ferguson et al., 1984; Zobell and Anderson, 1936)

4.2. Impact of dust addition under present environmental conditions

The addition of nitrogen and phosphorus in the experimental tanks through dust seeding (+ 11 to + 11.6 µmol L^{-1} and + 22 to + 30.8 nmol L^{-1} for NO_x and DIP, respectively, in dust enriched, i.e. D1 and D2, versus controls; Gazeau et al., 2020) had very contrasting impacts on the metabolism of the communities, depending on the station. At TYR, surprisingly, the relieving of nutrient limitation had a negative impact on ^{13}C incorporation as well as on both particulate and dissolved ^{14}C-based production rates (as seen by the relative changes compared to the control presented in Fig. 9). These observations are fully corroborated by the observed relative decrease in GPP in these tanks (D1 and D2) relative to controls and by the negative impact of dust-addition on TChl*a* concentrations as discussed by Gazeau et al. (2020). Integrated ^{14}C-

https://doi.org/10.5194/bg-2021-20
Preprint. Discussion started: 30 March 2021

675 incorporation rates converted to P (using a C:P molar ratio of 245:1 determined in the particulate
676 organic matter in surface waters of the Northwestern Mediterranean Sea during stratification;
677 Tanaka et al., 2011) showed that phytoplankton P requirements in treatment D (~2 nmol P L^{-1})
678 were much lower than the release of DIP through dust addition at this station (+ 20.4 to + 24.6
679 nmol P L^{-1}; Gazeau et al., 2020). This suggests that the observed strong decrease of DIP at this
680 station following dust addition was due to an utilization by the heterotrophic compartment.
681 Indeed, in contrast to the autotrophic compartment, both heterotrophic prokaryotic abundances
682 (Gazeau et al., 2020) and BP (this study, Fig. 9) showed that heterotrophic prokaryotes reacted
683 quickly and strongly to the increase in DIP availability. Integrated BP increased by almost 400%
684 in tanks D1 and D2 as compared to controls (Fig. 9). Such relative increases of BP surpassing by
685 far the observed relative increases of CR suggest a much more efficient utilization of resources
686 by heterotrophic prokaryotes in this treatment (i.e. BGE increased by 200% as compared to the
687 controls; Fig. 9). As such, at this station, the addition of dust drove the community to an even
688 more heterotrophic state. Such absence of response of the autotrophic community despite the
689 input of new N and P from simulated wet deposition was never observed in dust enrichment
690 experiments performed in the Mediterranean Sea (Guieu and Ridame, 2020). To the best of our
691 knowledge, it is the first time that a negative effect of dust addition is experimentally
692 demonstrated on the metabolic balance. The apparent utilization of nutrients, especially DIP
693 (Gazeau et al., 2020), by heterotrophic prokaryotes was extremely fast, starting right after dust
694 addition and driving DIP concentrations back to control levels at the end of the experiment
695 (t72h). While heterotrophic prokaryotic abundances increased until the end of the experiment,
696 BP rates increased exponentially during the fist 24h, and then BP reached a plateau.
697 Heterotrophic prokaryotes appeared limited by nutritive resources although DIP concentrations

https://doi.org/10.5194/bg-2021-20
Preprint. Discussion started: 30 March 2021

were not yet back to their initial level and no relative increase of the AP Vm per cell compared to the control was observed in these tanks. Independent nutrient experiments showed a direct stimulation of BP in the dark after addition of DIP (Van Wambeke et al., 2020b), suggesting a great competition with phytoplankton for DIP utilization at TYR. After 24 h, abundances of heterotrophic prokaryotes continued to increase while BP stabilized, suggesting a less extent of lysis and viral control than in the other experiments (abundances of heterotrophic nanoflagellates decreased; Dinasquet et al., 2021). This limitation of BP was potentially a consequence of relatively less available access to labile DOC sources, as ^{14}C-based production rates decreased relative to the controls at t24h and t48h although BP increased by 200 - 800%. The very tight coupling between phytoplankton and bacteria at all stations investigated was further confirmed by the absence of an important ^{13}C incorporation into DOC (Fig. S3).

At stations ION and FAST, in contrast to TYR, both the autotrophic and heterotrophic community benefited from dust addition relative to the controls (Fig. 9). Interestingly, while the relative increase in integrated autotrophic processes (GPP and all ^{14}C-based production rates) was more important at FAST than at ION, the opposite was observed for BP. Estimated BGE values even suggest an absence of response to dust addition at station FAST compared to the controls. The different (relative) responses of BP at the two stations could be partly explained by the dynamics of BP in the control tanks as no clear pattern could be observed at ION while a continuous increase was observed at FAST. As shown by Gazeau et al. (2020), at FAST, abundances of heterotrophic prokaryotes were much higher at the start of the experiment, further increased until t48h and then declined until the end of the experiment.

We can rule out a potential limitation of BP from DIP availability at station FAST as DIP levels remained much higher in tanks D than in the controls (Gazeau et al., 2020). Furthermore,

https://doi.org/10.5194/bg-2021-20
Preprint. Discussion started: 30 March 2021

721 the amount of maximum DIP reached before its decline compared to TYR and ION showed a
722 less important direct DIP uptake, suggesting that communities were not as much P limited at
723 FAST compared to the other stations at the start of the experiment. Finally, no increase of
724 specific AP Vm was observed in these tanks as compared to the controls (Fig. 7), suggesting no
725 particular additional needs for AP synthesis per unit cell following dust addition. A potential
726 explanation resides in the competition between heterotrophic bacteria and phytoplankton for DIP
727 utilization. At station ION, P requirements of the autotrophic community were low compared to
728 the initial input of DIP following dust seeding (~9 nmol P L^{-1} as compared to an input of + 22 to
729 + 23.3 nmol P L^{-1}; Gazeau et al., 2020). In contrast, at FAST, the autotrophic community
730 consumed a much larger proportion of the initial DIP input (~25 nmol P L^{-1} as compared to an
731 input of 30.8 - 31.3 nmol P L^{-1}) and phytoplankton appeared as a winner for the utilization of
732 DIP towards the end of the experiment at this station. It seems that heterotrophic bacteria and
733 phytoplankton were more in a steady state of equilibrium and less stressed at the start of the
734 experiment at FAST, i.e. phytoplankton abundances showed no decrease between t-12h and t0
735 and BP did not increase as much as during the other two experiments, suggesting a strong
736 predation pressure (μ_{BP} was the lowest of the three experiments: ca. 0.02 h^{-1} in the controls).

737 The explanation for the observed differential responses of the autotrophic community at
738 the two stations (FAST > ION) is not evident and further complicated by the fact that the
739 sampling strategy differed between the two stations (i.e. no sampling at t72h, replaced by a
740 sampling at t96h). It is however unlikely that this different sampling strategy was responsible for
741 the different changes in computed integrated autotrophic rates at the two stations. As a maximal
742 increase in nano-eukaryote abundance was observed at t72h at FAST (followed by a drastic
743 reduction at t96h; Gazeau et al., 2020), excluding this sampling point in the calculation of

https://doi.org/10.5194/bg-2021-20
Preprint. Discussion started: 30 March 2021

744 autotrophic metabolic rates would most likely have led to an underestimation of these rates rather
745 than an overestimation. Furthermore, a similar partitioning of ^{14}C-based production rates
746 throughout the two experiments did not provide clear insights on which size-group benefited the
747 most at station FAST compared to ION. Two non-exclusive explanations could be proposed: (1)
748 as mentioned above, a less important immediate consumption of DIP by heterotrophic bacteria
749 leading to a higher availability of new DIP for phytoplankton growth at FAST (+ 31 vs + 22 to +
750 23 nmol L^{-1} at FAST and ION, respectively; Gazeau et al., 2020) along with (2) the presence of a
751 potentially more active community at the start of the experiment at FAST with a much higher
752 contribution from smaller cells (i.e. pico-eukaryotes, *Synechococcus*; Gazeau et al., 2020) that
753 are well known to be better competitors for new nutrients and that were less stressed at the start
754 of the experiments (e.g. Moutin et al., 2002).

755 During both experiments at ION and FAST, communities switched from net heterotrophy
756 to net autotrophy between 48 and 72 h following dust addition (Fig. 6), leading to a positive
757 integrated NCP at both stations (Fig. 9). This is an important observation since, to the best of our
758 knowledge, the present study constitutes the first investigation of the community metabolism
759 response to dust addition. However, it is important to discuss the timing of such a switch in
760 community metabolism. Since heterotrophic prokaryotes reacted faster than autotrophs to the
761 relief of nutrient limitation (i.e. BP already increased by 150-500% at t24 h, while ^{14}C-based
762 production rates increased only after 48-72 h), NCP was first lower (and negative) in the dust-
763 amended tanks as compared to the controls. Marañón et al. (2010) and Pulido-Villena (2008,
764 2014) have already reported on a much faster response of the heterotrophic prokaryote
765 community to dust enrichment in the central Atlantic Ocean and Mediterranean Sea,
766 respectively. As DIP concentrations at the completion of their 48 h incubations did not differ

https://doi.org/10.5194/bg-2021-20
Preprint. Discussion started: 30 March 2021

767 from that in the controls, it is unlikely that primary production rates and consequently NCP
768 would have further increased. In contrast, during our experiments, DIP concentrations in dust-
769 amended tanks (D) reached initial levels only after 72 h at TYR and ION and remained far above
770 ambient levels at FAST until the end of the experiment (t96h). During the PEACETIME cruise,
771 high frequency sampling of CTD casts allowed following the evolution of biogeochemical
772 properties and fluxes before and after wet dust deposition that took place in the area around
773 FAST on June 3-5 (Van Wambeke et al., 2020a). As in our experiment, a rapid increase in BP
774 was responsible for the observed *in situ* decline in DIP concentrations in the mixed layer
775 following the rain with no detectable changes in primary production (Van Wambeke et al.,
776 2020a). The intensity of the wet deposition event that was simulated during our experiments was,
777 by far, more important, but still representative of a realistic scenario (Bonnet and Guieu, 2006;
778 Loÿe-Pilot and Martin, 1996; Ternon et al., 2010).

779 The most intriguing result concerning the export of inorganic and organic matter is that
780 these fluxes were maximal at the end of the experiment at TYR in the dust-amended tanks
781 despite the fact that ^{14}C-based production was relatively low and not enhanced by dust addition.
782 Based on previous studies (Bressac et al., 2014; Louis et al., 2017; Ternon et al., 2010), organic
783 matter export was most likely mainly due to the formation of organic-mineral aggregates
784 triggered by the introduced lithogenic particles (referred thereafter to as POC_{litho}). Indeed, Louis
785 et al. (2017) showed that such an aggregation process occurs within 1 h after dust deposition.
786 These authors further demonstrated the key role of TEP as the conversion of dissolved organic
787 matter (DOM) to POC was mediated by TEP formation/aggregation activated by the introduction
788 of dust. As TEP concentrations were only measured on two occasions after seeding with the first
789 measurement occuring at t24h,), it prevents studying in detail the dynamics of these particles.

https://doi.org/10.5194/bg-2021-20
Preprint. Discussion started: 30 March 2021

790 Nevertheless, it is very likely that the sharp decrease of TEP abundances (data not shown)
791 between t24h and t72h was related to POC_{litho} export. The coefficient linking POC_{litho} to $Litho_{flux}$
792 (i.e. the mass of sedimented particles) measured here (0.02) is consistent with values reported for
793 other experiments conducted in the Mediterranean Sea (Louis et al., 2017).

794 Even though ^{14}C-based production rates were enhanced in the dust-amended tanks at
795 stations ION and FAST, the amount of POC exported at the end of these experiments remained
796 lower than at TYR, with fluxes ~ 10-20 mg C m^{-2} d^{-1}. It must be stressed that not all the
797 lithogenic material introduced in the tanks was recovered after 4 (and 5) days, with the highest
798 percentage (~ 30%) being found at TYR, indicating that the tested waters at this station had a
799 better capacity to aggregate dust. This efficiency to export POC_{litho} more rapidly at TYR
800 compared to ION and FAST was likely due to the age and quantity of dissolved organic matter
801 present at the time of the seeding (Bressac and Guieu, 2013). At TYR, impacted by a strong dust
802 event several days before the experiment started (see above), the likely stimulation of the
803 autotrophs after this *in situ* event should have been followed by the production of a fresh and
804 abundant DOM, comparable to the "post-bloom situation" in Bressac and Guieu (2013).

805 4.3. Impact of dust addition under future environmental
806 conditions

807 Warming and/or acidification had a clear impact on most evaluated stocks and metabolic
808 rates. Gazeau et al. (2020) have already discussed temperature/pH mediated changes in nutrient
809 uptake rates and autotrophic community composition in these experiments. The difference in the
810 relative response of plankton communities to dust addition under present and future conditions of
811 temperature and pH was highly dependent on the sampling station (Fig. 9). At all stations, ^{14}C-

https://doi.org/10.5194/bg-2021-20
Preprint. Discussion started: 30 March 2021

based particulate production rates were enhanced under future conditions as compared to those measured under present environmental conditions (treatment D) although this pattern was not observed for ^{13}C incorporation into POC at stations ION and FAST. At ION, no differences could be detected and at FAST an even lower ^{13}C-enrichment was measured at the end of the experiment. These contrasting patterns between ^{14}C-uptake rates and ^{13}C-enrichment of POC are likely explained by the fact that the latter covered the whole experimental period (including dark periods) and represents net community carbon production while ^{14}C-based rates were measured over 8 h incubations in the light, providing an estimate in between gross and net carbon production.

Similarly, the heterotrophic compartment was more stimulated, as BP rates increased strongly at all stations under this treatment compared to treatment D. The relatively smaller increase in CR rates, compared to BP, leading to higher BGE suggests a better utilization of resources by heterotrophic prokaryotes under future environmental conditions. Overall, CR was more impacted than GPP, with the consequence that all integrated NCP rates decreased under future environmental conditions compared to present conditions (treatment D). At station TYR, as discussed previously, dust addition under present conditions did not lead to a switch from net heterotrophy to net autotrophy. This pattern was even more obvious under warmer/acidified conditions, with a larger decrease in integrated NCP at this station. The decrease of integrated NCP at station FAST relative to controls, as well as the smaller increase of all ^{14}C-based production rates relative to those observed at station ION must be taken with caution. As already discussed, the fact that for these processes (O_2 metabolism and ^{14}C-incorporation), no samples were taken at FAST at t72h when maximal cell abundances were recorded for all autotrophic groups (pico- and nano-eukaryotes, autotrophic bacteria) must have artificially led to an

https://doi.org/10.5194/bg-2021-20
Preprint. Discussion started: 30 March 2021

underestimation of these integrated metabolic rates. The question of the timing appeared even more preponderant under warmer/acidified conditions, especially at station FAST, where the very important increase in BP led to a full consumption of DIP before t48h (Gazeau et al., 2020) and drove the community towards a strong heterotrophy. The metabolic balance further switched to a slight autotrophy at t72h when heterotrophic bacterial activity appeared limited by nutrient availability.

Both elevated partial pressure of CO_2 (pCO_2) and warming are major global change stressors impacting marine communities. Elevated pCO_2 may directly facilitate oceanic primary production through enhanced photosynthesis (Hein and Sand-Jensen, 1997; Riebesell et al., 2007) although the effects appear to be species- and even strain-specific (e.g. Langer et al., 2009). Warming affects organisms by enhancing their metabolic rates (Brown et al., 2004; Gillooly et al., 2001). Although recent studies suggest large differences in temperature sensitivity between phytoplankton taxa (Chen and Laws, 2017) and no significant overall difference between algae and protozoa (Wang et al., 2019), mineralization rates are usually believed to be more impacted by warming than primary production rates, potentially leading to a decline in net oceanic carbon fixation (Boscolo-Galazzo et al., 2018; Garcia-Corral et al., 2017; Lopez-Urrutia and Moran, 2007; Regaudie-de-Gioux and Duarte, 2012) and carbon export efficiency (Cael et al., 2017; Cael and Follows, 2016). Overall, our experimental set-up did not allow discriminating warming from acidification effects, precluding an evaluation of their potential individual impacts. Nevertheless, we could speculate to which extent a 3 ºC warming and a doubling of CO_2 can explain some of the observed differences between D and G (for instance, a 2-fold increase in ^{14}C-based production rates at ION). For photosynthesis, meta-analysis studies indicate minor effects of pCO_2 on most investigated species (Kroeker et al., 2013; Mackey et al.,

https://doi.org/10.5194/bg-2021-20
Preprint. Discussion started: 30 March 2021

858 2015). Recent studies show a strong, although species-dependent, temperature sensitivity of
859 phytoplankton growth (Chen and Laws, 2017; Wang et al., 2019), suggesting that a 3 ºC
860 warming could explain most of the increased carbon fixation in G compared to D. With respect
861 to NCP, our results are in line with the general view and suggest a weakening of the so-called
862 fertilization effect of atmospheric deposition in the coming decades.

863 In contrast, we did not observe an additional impact of future environmental conditions
864 on the export of organic matter after dust addition as, at each station, this export was of the same
865 order of magnitude for treatments D and G. This result is in agreement with the findings of a
866 similar experiment in coastal Mediterranean waters that considered only pH change (Louis et al.,
867 2017) but stands in contrast with the findings of Müren et al. (2005) who showed a clear
868 decrease in sedimentation following a 5 °C warming in the Baltic Sea. Only a few studies have
869 addressed the combined effect of both temperature and pH changes on aggregation processes and
870 export but none considered dust as the particulate phase. These studies, focused mainly on the
871 formation of TEP, were inconclusive on the impact of these combined factors (Passow and
872 Carlson, 2012, and references therein). As the potential effect of warming and acidification on
873 biogenic carbon export was certainly, over the rather restricted duration of the experiments,
874 insignificant as compared to the large amount of carbon exported through the lithogenic pump,
875 observations over longer temporal scales are probably required to ascertain the interactive effects
876 of these stressors in the coming decades.

https://doi.org/10.5194/bg-2021-20
Preprint. Discussion started: 30 March 2021

5. Conclusion

Although the three experiments were conducted under rather similar conditions in terms of nutrient availability and chlorophyll stock of the tested seawater, contrasting responses were observed following the simulation of a wet dust deposition event. Under present conditions of temperature and pH, at the site where the community was the most heterotrophic (TYR), no positive impact of new nutrients could be observed on autotrophs, while a fast and strong response of heterotrophic bacteria drove the metabolic balance towards an even more heterotrophic state. The situation was different at the two other stations where a more active autotrophic community responded quickly to the relief in nutrient limitation, driving the community to an autotrophic state at the end of these experiments. In all tested waters, an overall faster response of the heterotrophic prokaryote community, as compared to the autotrophic community, was observed after new nutrients were released from dust. Phytoplankton could benefit from nutrient inputs, only if the amount released from dust was enough to sustain both the fast bacterial demand and the delayed one of phytoplankton. As our experimental protocol consisted in simulating a strong, although realistic, wet dust deposition, further work should explore at which flux a wet dust deposition triggers an enhancement of net community production and therefore increases the capacity of the surface oligotrophic ocean to sequester atmospheric CO_2. This question, of the utmost importance in particular for modelling purposes, should be answered through future similar experiments as the ones considered in our study but following a gradient approach of dust fluxes. As a consequence of a stronger sensitivity of heterotrophic prokaryotes to temperature and/or pH, the ongoing warming and acidification of the surface ocean will result in a decrease of the dust fertilization of phytoplankton in the coming decades and a weakening the CO_2 sequestration capacity of the surface oligotrophic ocean.

https://doi.org/10.5194/bg-2021-20
Preprint. Discussion started: 30 March 2021

900 # Data availability

901 All data and metadata will be made available at the French INSU/CNRS LEFE CYBER database
902 (scientific coordinator: Hervé Claustre; data manager, webmaster: Catherine Schmechtig).
903 INSU/CNRS LEFE CYBER (2020)

904 # Author contributions

905 FG and CG designed and supervised the study. All authors participated in sample analyses. FG
906 wrote the paper with contributions from all authors.

907 # Financial support

908 This study is a contribution to the PEACETIME project (http://peacetime-project.org), a joint
909 initiative of the MERMEX and ChArMEx components supported by CNRS-INSU, IFREMER,
910 CEA, and Météo-France as part of the programme MISTRALS coordinated by INSU.
911 PEACETIME was endorsed as a process study by GEOTRACES and is a contribution to IMBER
912 and SOLAS International programs. PEACETIME cruise (https://doi.org/10.17600/17000300).
913 The project leading to this publication has received funding from European FEDER Fund under
914 project 1166-39417. The research of EM and MPL was supported by the Spanish Ministry of
915 Science, Innovation and Universities through project POLARIS (Grant No. PGC2018-094553B-
916 I00) and by European Union's H2020 research and innovation programme through project
917 TRIATLAS (Grant No. 817578). JD was funded by a Marie Curie Actions-International
918 Outgoing Fellowship (PIOF-GA-2013-629378).

919

https://doi.org/10.5194/bg-2021-20
Preprint. Discussion started: 30 March 2021

Acknowledgments

The authors thank the captain and the crew of the RV “Pourquoi Pas ?” for their professionalism and their work at sea. Céline Ridame and Kahina Djaoudi are thanked for their help during sampling, Sophie Guasco and Marc Garel for their help in ectoenzymatic measurements onboard.

https://doi.org/10.5194/bg-2021-20
Preprint. Discussion started: 30 March 2021

References

Behrenfeld, M. J., O'Malley, R. T., Siegel, D. A., McClain, C. R., Sarmiento, J. L., Feldman, G. C., Milligan, A. J., Falkowski, P. G., Letelier, R. M. and Boss, E. S.: Climate-driven trends in contemporary ocean productivity, Nature, 444(7120), 752–755, 2006.

Benner, R. and Strom, M.: A critical evaluation of the analytical blank associated with DOC measurements by high-temperature catalytic oxidation, Marine Chemistry, 41(1), 153–160, https://doi.org/10.1016/0304-4203(93)90113-3, 1993.

Bergametti, Gi., Dutot, A.-L., Buat-Ménard, P., Losno, R. and Remoudaki, E.: Seasonal variability of the elemental composition of atmospheric aerosol particles over the Northwestern Mediterranean, Tellus B: Chemical and Physical Meteorology, 41(3), 353–361, https://doi.org/10.3402/tellusb.v41i3.15092, 1989.

Bishop, J. K. B., Davis, R. E. and Sherman, J. T.: Robotic Observations of Dust Storm Enhancement of Carbon Biomass in the North Pacific, Science, 298(5594), 817–821, https://doi.org/10.1126/science.1074961, 2002.

Bonnet, S. and Guieu, C.: Atmospheric forcing on the annual iron cycle in the western Mediterranean Sea: A 1-year survey, Journal of Geophysical Research: Oceans, 111(C9), https://doi.org/10.1029/2005JC003213, 2006.

Bonnet, S., Guieu, C., Chiaverini, J., Ras, J. and Stock, A.: Effect of atmospheric nutrients on the autotrophic communities in a low nutrient, low chlorophyll system, Limnology and Oceanography, 50(6), 1810–1819, https://doi.org/10.4319/lo.2005.50.6.1810, 2005.

Bosc, E., Bricaud, A. and Antoine, D.: Seasonal and interannual variability in algal biomass and primary production in the Mediterranean Sea, as derived from 4 years of SeaWiFS observations, Global Biogeochemical Cycles, 18(1),

https://doi.org/10.1029/2003GB002034, 2004.

Boscolo-Galazzo, F., Crichton, K. A., Barker, S. and Pearson, P. N.: Temperature dependency of metabolic rates in the upper ocean: A positive feedback to global climate change?, Global and Planetary Change, 170, 201–212, https://doi.org/10.1016/j.gloplacha.2018.08.017, 2018.

Bressac, M. and Guieu, C.: Post-depositional processes: What really happens to new atmospheric iron in the ocean's surface?, Global Biogeochemical Cycles, 27(3), 859–870, https://doi.org/10.1002/gbc.20076, 2013.

Bressac, M., Guieu, C., Doxaran, D., Bourrin, F., Desboeufs, K., Leblond, N. and Ridame, C.: Quantification of the lithogenic carbon pump following a simulated dust-deposition event in large mesocosms, Biogeosciences, 11(4), 1007–1020, https://doi.org/10.5194/bg-11-1007-2014, 2014.

Brown, J. H., Gillooly, J. F., Allen, A. P., Savage, V. M. and West, G. B.: Toward a Metabolic Theory of Ecology, Ecology, 85(7), 1771–1789, https://doi.org/10.1890/03-9000, 2004.

Cael, B. B. and Follows, M. J.: On the temperature dependence of oceanic export efficiency, Geophysical Research Letters, 43(10), 5170–5175, https://doi.org/10.1002/2016GL068877, 2016.

Cael, B. B., Bisson, K. and Follows, M. J.: How have recent temperature changes affected the efficiency of ocean biological carbon export?, Limnology and Oceanography Letters, 2(4), 113–118, https://doi.org/10.1002/lol2.10042, 2017.

Calvo-Díaz, A., Díaz-Pérez, L., Suárez, L. Á., Morán, X. A. G., Teira, E. and Marañón, E.: Decrease in the Autotrophic-to-Heterotrophic Biomass Ratio of Picoplankton in Oligotrophic Marine Waters Due to Bottle Enclosure, Appl. Environ. Microbiol., 77(16),

https://doi.org/10.5194/bg-2021-20
Preprint. Discussion started: 30 March 2021

5739–5746, https://doi.org/10.1128/AEM.00066-11, 2011.

Chen, B. and Laws, E. A.: Is there a difference of temperature sensitivity between marine phytoplankton and heterotrophs?, Limnology and Oceanography, 62(2), 806–817, https://doi.org/10.1002/lno.10462, 2017.

Christaki, U., Van Wambeke, F., Lefevre, D., Lagaria, A., Prieur, L., Pujo-Pay, M., Grattepanche, J.-D., Colombet, J., Psarra, S., Dolan, J. R., Sime-Ngando, T., Conan, P., Weinbauer, M. G. and Moutin, T.: Microbial food webs and metabolic state across oligotrophic waters of the Mediterranean Sea during summer, Biogeosciences, 8(7), 1839–1852, https://doi.org/10.5194/bg-8-1839-2011, 2011.

Desboeufs, K., Leblond, N., Wagener, T., Bon Nguyen, E. and Guieu, C.: Chemical fate and settling of mineral dust in surface seawater after atmospheric deposition observed from dust seeding experiments in large mesocosms, Biogeosciences, 11(19), 5581–5594, https://doi.org/10.5194/bg-11-5581-2014, 2014.

Desboeufs, K., Bon Nguyen, E., Chevaillier, S., Triquet, S. and Dulac, F.: Fluxes and sources of nutrient and trace metal atmospheric deposition in the Northwestern Mediterranean, Atmospheric Chemistry and Physics, 18(19), 14477–14492, https://doi.org/10.5194/acp-18-14477-2018, 2018.

Dinasquet, J., Bigeard, E., Gazeau, F., Marañón, E., Ridame, C., Van Wambeke, F., Obernosterer, I. and Baudoux, A.-C.: Impact of dust enrichment on the microbial food web under present and future conditions of pH and temperature, Biogeosciences Discussions, 2021.

Dittmar, T., Cherrier, J. and Ludwichowski, K.-U.: The analysis of amino acids in seawater, in Practical Guidelines for the Analysis of Seawater, edited by O. Wurl, pp. 67–77, CRC

https://doi.org/10.5194/bg-2021-20
Preprint. Discussion started: 30 March 2021

993 Press Taylor & Francis Group, Boca Raton, FL., , 2009.
994 Emerson, S., Quay, P., Karl, D., Winn, C., Tupas, L. and Landry, M.: Experimental
995 determination of the organic carbon flux from open-ocean surface waters, Nature,
996 389(6654), 951–954, https://doi.org/10.1038/40111, 1997.
997 Engel, A.: Determination of marine gel particles, in Practical Guidelines for the Analysis of
998 Seawater, edited by O. Wurl, pp. 125–142, CRC Press Taylor & Francis Group, Boca
999 Raton, FL., , 2009.
1000 Engel, A. and Händel, N.: A novel protocol for determining the concentration and composition
1001 of sugars in particulate and in high molecular weight dissolved organic matter (HMW-
1002 DOM) in seawater, Marine Chemistry, 127(1), 180–191,
1003 https://doi.org/10.1016/j.marchem.2011.09.004, 2011.
1004 Feliú, G., Pagano, M., Hidalgo, P. and Carlotti, F.: Structure and function of epipelagic
1005 mesozooplankton and their response to dust deposition events during the spring
1006 PEACETIME cruise in the Mediterranean Sea, Biogeosciences, 17, 5417–5441,
1007 https://doi.org/10.5194/bg-17-5417-2020, 2020.
1008 Ferguson, R. L., Buckley, E. N. and Palumbo, A. V.: Response of marine bacterioplankton to
1009 differential filtration and confinement., Appl. Environ. Microbiol., 47(1), 49–55, 1984.
1010 Friedlingstein, P., O'Sullivan, M., Jones, M. W., Andrew, R. M., Hauck, J., Olsen, A., Peters, G.
1011 P., Peters, W., Pongratz, J., Sitch, S., Le Quéré, C., Canadell, J. G., Ciais, P., Jackson, R.
1012 B., Alin, S., Aragão, L. E. O. C., Arneth, A., Arora, V., Bates, N. R., Becker, M., Benoit-
1013 Cattin, A., Bittig, H. C., Bopp, L., Bultan, S., Chandra, N., Chevallier, F., Chini, L. P.,
1014 Evans, W., Florentie, L., Forster, P. M., Gasser, T., Gehlen, M., Gilfillan, D., Gkritzalis,
1015 T., Gregor, L., Gruber, N., Harris, I., Hartung, K., Haverd, V., Houghton, R. A., Ilyina,

https://doi.org/10.5194/bg-2021-20
Preprint. Discussion started: 30 March 2021

T., Jain, A. K., Joetzjer, E., Kadono, K., Kato, E., Kitidis, V., Korsbakken, J. I., Landschützer, P., Lefèvre, N., Lenton, A., Lienert, S., Liu, Z., Lombardozzi, D., Marland, G., Metzl, N., Munro, D. R., Nabel, J. E. M. S., Nakaoka, S.-I., Niwa, Y., O'Brien, K., Ono, T., Palmer, P. I., Pierrot, D., Poulter, B., Resplandy, L., Robertson, E., Rödenbeck, C., Schwinger, J., Séférian, R., Skjelvan, I., Smith, A. J. P., Sutton, A. J., Tanhua, T., Tans, P. P., Tian, H., Tilbrook, B., van der Werf, G., Vuichard, N., Walker, A. P., Wanninkhof, R., Watson, A. J., Willis, D., Wiltshire, A. J., Yuan, W., Yue, X. and Zaehle, S.: Global Carbon Budget 2020, Earth System Science Data, 12(4), 3269–3340, https://doi.org/10.5194/essd-12-3269-2020, 2020.

Garcia-Corral, L. S., Holding, J. M., Carrillo-de-Albornoz, P., Steckbauer, A., Pérez-Lorenzo, M., Navarro, N., Serret, P., Gasol, J. M., Morán, X. A. G., Estrada, M., Fraile-Nuez, E., Benítez-Barrios, V., Agusti, S. and Duarte, C. M.: Temperature dependence of plankton community metabolism in the subtropical and tropical oceans, Global Biogeochemical Cycles, 31(7), 1141–1154, https://doi.org/10.1002/2017GB005629, 2017.

Gazeau, F., Ridame, C., Van Wambeke, F., Alliouane, S., Stolpe, C., Irisson, J.-O., Marro, S., Grisoni, J.-M., De Liège, G., Nunige, S., Djaoudi, K., Pulido-Villena, E., Dinasquet, J., Obernosterer, I., Catala, P. and Guieu, C.: Impact of dust enrichment on Mediterranean plankton communities under present and future conditions of pH and temperature: an overview, Biogeosciences Discussions, https://doi.org/10.5194/bg-2020-202, 2020.

Gillikin, D. P. and Bouillon, S.: Determination of δ18O of water and δ13C of dissolved inorganic carbon using a simple modification of an elemental analyser-isotope ratio mass spectrometer: an evaluation, Rapid Communications in Mass Spectrometry, 21(8), 1475–1478, https://doi.org/10.1002/rcm.2968, 2007.

https://doi.org/10.5194/bg-2021-20
Preprint. Discussion started: 30 March 2021

1039 Gillooly, J. F., Brown, J. H., West, G. B., Savage, V. M. and Charnov, E. L.: Effects of Size and
1040 Temperature on Metabolic Rate, Science, 293(5538), 2248–2251,
1041 https://doi.org/10.1126/science.1061967, 2001.
1042 del Giorgio, P. and Williams, P.: Respiration in Aquatic Ecosystems, Oxford University Press.
1043 https://oxford.universitypressscholarship.com/view/10.1093/acprof:oso/9780198527084.
1044 001.0001/acprof-9780198527084, last access: 22 January 2021, 2005.
1045 Guieu, C. and Ridame, C.: Impact of atmospheric deposition on marine chemistry and
1046 biogeochemistry, in Atmospheric Chemistry in the Mediterranean Region:
1047 Comprehensive Diagnosis and Impacts, edited by F. Dulac, S. Sauvage, and E. Hamonou,
1048 Springer, Cham, Switzerland, , 2020.
1049 Guieu, C., Loye-Pilot, M. D., Benyahya, L. and Dufour, A.: Spatial variability of atmospheric
1050 fluxes of metals (Al, Fe, Cd, Zn and Pb) and phosphorus over the whole Mediterranean
1051 from a one-year monitoring experiment: Biogeochemical implications, Marine
1052 Chemistry, 120(1–4), 164–178, https://doi.org/10.1016/j.marchem.2009.02.004, 2010.
1053 Guieu, C., Ridame, C., Pulido-Villena, E., Bressac, M., Desboeufs, K. and Dulac, F.: Impact of
1054 dust deposition on carbon budget: a tentative assessment from a mesocosm approach,
1055 Biogeosciences, 11(19), 5621–5635, 2014a.
1056 Guieu, C., Aumont, O., Paytan, A., Bopp, L., Law, C. S., Mahowald, N., Achterberg, E. P.,
1057 Marañón, E., Salihoglu, B., Crise, A., Wagener, T., Herut, B., Desboeufs, K., Kanakidou,
1058 M., Olgun, N., Peters, F., Pulido-Villena, E., Tovar-Sanchez, A. and Völker, C.: The
1059 significance of the episodic nature of atmospheric deposition to Low Nutrient Low
1060 Chlorophyll regions, Global Biogeochemical Cycles, 28(11), 1179–1198,
1061 https://doi.org/10.1002/2014GB004852, 2014b.

https://doi.org/10.5194/bg-2021-20
Preprint. Discussion started: 30 March 2021

1062 Guieu, C., D'Ortenzio, F., Dulac, F., Taillandier, V., Doglioli, A., Petrenko, A., Barrillon, S.,
1063 Mallet, M., Nabat, P. and Desboeufs, K.: Process studies at the air-sea interface after
1064 atmospheric deposition in the Mediterranean Sea: objectives and strategy of the
1065 PEACETIME oceanographic campaign (May–June 2017), Biogeosciences, 2020(17),
1066 5563–5585, https://doi.org/10.5194/bg-17-5563-2020, 2020.
1067 Hein, M. and Sand-Jensen, K.: CO2 increases oceanic primary production, Nature, 388(6642),
1068 526–527, 1997.
1069 Herut, B., Zohary, T., Krom, M. D., Mantoura, R. F. C., Pitta, P., Psarra, S., Rassoulzadegan, F.,
1070 Tanaka, T. and Frede Thingstad, T.: Response of East Mediterranean surface water to
1071 Saharan dust: On-board microcosm experiment and field observations, Deep Sea
1072 Research Part II: Topical Studies in Oceanography, 52(22), 3024–3040,
1073 https://doi.org/10.1016/j.dsr2.2005.09.003, 2005.
1074 Herut, B., Rahav, E., Tsagaraki, T. M., Giannakourou, A., Tsiola, A., Psarra, S., Lagaria, A.,
1075 Papageorgiou, N., Mihalopoulos, N., Theodosi, C. N., Violaki, K., Stathopoulou, E.,
1076 Scoullos, M., Krom, M. D., Stockdale, A., Shi, Z., Berman-Frank, I., Meador, T. B.,
1077 Tanaka, T. and Paraskevi, P.: The Potential Impact of Saharan Dust and Polluted
1078 Aerosols on Microbial Populations in the East Mediterranean Sea, an Overview of a
1079 Mesocosm Experimental Approach, Front. Mar. Sci., 3,
1080 https://doi.org/10.3389/fmars.2016.00226, 2016.
1081 Hoppe, H.-G.: Significance of exoenzymatic activities in the ecology of brackish water:
1082 measurements by means of methylumbelliferyl-substrates, Marine Ecology Progress
1083 Series, 11(3), 299–308, 1983.
1084 IPCC: Climate Change, The Physical Science Basis., 2013.

https://doi.org/10.5194/bg-2021-20
Preprint. Discussion started: 30 March 2021

1085 Irwin, A. J. and Oliver, M. J.: Are ocean deserts getting larger?, Geophysical Research Letters,
1086 36, https://doi.org/10.1029/2009gl039883, 2009.
1087 Jickells, T. and Moore, C. M.: The Importance of Atmospheric Deposition for Ocean
1088 Productivity, Annual Review of Ecology, Evolution, and Systematics, 46(1), 481–501,
1089 https://doi.org/10.1146/annurev-ecolsys-112414-054118, 2015.
1090 Kirchman, D. L., Kemp, P., Sherr, B., Sherr, E. and Cole, J.: Leucine Incorporation as a Measure
1091 of Biomass Production by Heterotrophic Bacteria, in Handbook of Methods in Aquatic
1092 Microbial Ecology, pp. 509–512, CRC Press, https://doi.org/10.1201/9780203752746-59,
1093 , 1993.
1094 Knap, A., Michaels, A., Close, A., Ducklow, H. and Dickson, A.: Protocols for the Joint Global
1095 Ocean Flux Study (JGOFS) Core Measurements, UNESCO 1994., 1996.
1096 Kouvarakis, G., Mihalopoulos, N., Tselepides, A. and Stavrakakis, S.: On the importance of
1097 atmospheric inputs of inorganic nitrogen species on the productivity of the Eastern
1098 Mediterranean Sea, Global Biogeochemical Cycles, 15(4), 805–817,
1099 https://doi.org/10.1029/2001GB001399, 2001.
1100 Kroeker, K. J., Kordas, R. L., Crim, R., Hendriks, I. E., Ramajo, L., Singh, G. S., Duarte, C. M.
1101 and Gattuso, J. P.: Impacts of ocean acidification on marine organisms: quantifying
1102 sensitivities and interaction with warming, Global Change Biology, 19(6), 1884–1896,
1103 https://doi.org/10.1111/gcb.12179, 2013.
1104 Langer, G., Nehrke, G., Probert, I., Ly, J. and Ziveri, P.: Strain-specific responses of *Emiliania*
1105 *huxleyi* to changing seawater carbonate chemistry, Biogeosciences, 6(11), 2637–2646,
1106 https://doi.org/10.5194/bg-6-2637-2009, 2009.
1107 Laurent, B., Audoux, T., Bibi, M., Dulac, F. and Bergametti, G.: Mass deposition in the

https://doi.org/10.5194/bg-2021-20
Preprint. Discussion started: 30 March 2021

Mediterranean region, in Atmospheric Chemistry in the Mediterranean Region: Comprehensive Diagnosis and Impacts, edited by F. Dulac, S. Sauvage, and E. Hamonou, Springer, Cham, Switzerland, , 2021.

Lazzari, P., Solidoro, C., Salon, S. and Bolzon, G.: Spatial variability of phosphate and nitrate in the Mediterranean Sea: A modeling approach, Deep Sea Research Part I: Oceanographic Research Papers, 108, 39–52, https://doi.org/10.1016/j.dsr.2015.12.006, 2016.

Lekunberri, I., Lefort, T., Romero, E., Vázquez-Domínguez, E., Romera-Castillo, C., Marrasé, C., Peters, F., Weinbauer, M. and Gasol, J. M.: Effects of a dust deposition event on coastal marine microbial abundance and activity, bacterial community structure and ecosystem function, J Plankton Res, 32(4), 381–396, https://doi.org/10.1093/plankt/fbp137, 2010.

Lemée, R., Rochelle-Newall, E., Van Wambeke, F., Pizay, M., Rinaldi, P. and Gattuso, J.: Seasonal variation of bacterial production, respiration and growth efficiency in the open NW Mediterranean Sea, Aquat. Microb. Ecol., 29, 227–237, https://doi.org/10.3354/ame029227, 2002.

Lewandowska, A. M., Boyce, D. G., Hofmann, M., Matthiessen, B., Sommer, U. and Worm, B.: Effects of sea surface warming on marine plankton, Ecology Letters, 17(5), 614–623, https://doi.org/10.1111/ele.12265, 2014.

Lindroth, P. and Mopper, K.: High performance liquid chromatographic determination of subpicomole amounts of amino acids by precolumn fluorescence derivatization with o-phthaldialdehyde, Anal. Chem., 51(11), 1667–1674, https://doi.org/10.1021/ac50047a019, 1979.

Longhurst, A., Sathyendranath, S., Platt, T. and Caverhill, C.: An estimate of global primary

https://doi.org/10.5194/bg-2021-20
Preprint. Discussion started: 30 March 2021

production in the ocean from satellite radiometer data, Journal of Plankton Research, 17(6), 1245–1271, https://doi.org/10.1093/plankt/17.6.1245, 1995.

Lopez-Urrutia, A. and Moran, X. A. G.: Resource limitation of bacterial production distorts the temperature dependence of oceanic carbon cycling, Ecology, 88(4), 817–822, 2007.

Louis, J., Pedrotti, M. L., Gazeau, F. and Guieu, C.: Experimental evidence of formation of transparent exopolymer particles (TEP) and POC export provoked by dust addition under current and high pCO_2 conditions, PLOS ONE, 12(2), e0171980, https://doi.org/10.1371/journal.pone.0171980, 2017.

Loÿe-Pilot, M. D. and Martin, J. M.: Saharan Dust Input to the Western Mediterranean: An Eleven Years Record in Corsica, in The Impact of Desert Dust Across the Mediterranean, edited by S. Guerzoni and R. Chester, pp. 191–199, Springer Netherlands, Dordrecht, https://doi.org/10.1007/978-94-017-3354-0_18, , 1996.

Mackey, K., Morris, J. J., Morel, F. and Kranz, S.: Response of photosynthesis to ocean acidification, Oceanography, 25(2), 74–91, https://doi.org/10.5670/oceanog.2015.33, 2015.

Marañón, E., Fernández, A., Mouriño-Carballido, B., MartÍnez-GarcÍa, S., Teira, E., Cermeño, P., Chouciño, P., Huete-Ortega, M., Fernández, E., Calvo-DÍaz, A., Morán, X. A. G., Bode, A., Moreno-Ostos, E., Varela, M. M., Patey, M. D. and Achterberg, E. P.: Degree of oligotrophy controls the response of microbial plankton to Saharan dust, Limnology and Oceanography, 55(6), 2339–2352, https://doi.org/10.4319/lo.2010.55.6.2339, 2010.

Marañón, E., Lorenzo, M. P., Cermeño, P. and Mouriño-Carballido, B.: Nutrient limitation suppresses the temperature dependence of phytoplankton metabolic rates, The ISME Journal, 12(7), 1836–1845, https://doi.org/10.1038/s41396-018-0105-1, 2018.

https://doi.org/10.5194/bg-2021-20
Preprint. Discussion started: 30 March 2021

1154 Marañón, E., Van Wambeke, F., Uitz, J., Boss, E. S., Pérez-Lorenzo, M., Dinasquet, J.,
1155 Haëntjens, N., Dimier, C. and Taillandier, V.: Deep maxima of phytoplankton biomass,
1156 primary production and bacterial production in the Mediterranean Sea during late spring,
1157 Biogeosciences Discussions, 1–28, https://doi.org/10.5194/bg-2020-261, 2020.
1158 Mari, X.: Carbon content and C:N ratio of transparent exopolymeric particles (TEP) produced by
1159 bubbling exudates of diatoms, Marine Ecology Progress Series, 183, 59–71,
1160 https://doi.org/10.3354/meps183059, 1999.
1161 Markaki, Z., Oikonomou, K., Kocak, M., Kouvarakis, G., Chaniotaki, A., Kubilay, N. and
1162 Mihalopoulos, N.: Atmospheric deposition of inorganic phosphorus in the Levantine
1163 Basin, eastern Mediterranean: Spatial and temporal variability and its role in seawater
1164 productivity, Limnology and Oceanography, 48(4), 1557–1568,
1165 https://doi.org/10.4319/lo.2003.48.4.1557, 2003.
1166 Maugendre, L., Gattuso, J.-P., Louis, J., de Kluijver, A., Marro, S., Soetaert, K. and Gazeau, F.:
1167 Effect of ocean warming and acidification on a plankton community in the NW
1168 Mediterranean Sea, ICES Journal of Marine Science: Journal du Conseil, 72(6), 1744–
1169 1755, https://doi.org/10.1093/icesjms/fsu161, 2015.
1170 Maugendre, L., Gattuso, J.-P., Poulton, A. J., Dellisanti, W., Gaubert, M., Guieu, C. and Gazeau,
1171 F.: No detectable effect of ocean acidification on plankton metabolism in the NW
1172 oligotrophic Mediterranean Sea: Results from two mesocosm studies, Estuarine, Coastal
1173 and Shelf Science, 186, 89–99, https://doi.org/10.1016/j.ecss.2015.03.009, 2017a.
1174 Maugendre, L., Guieu, C., Gattuso, J.-P. and Gazeau, F.: Ocean acidification in the
1175 Mediterranean Sea: Pelagic mesocosm experiments. A synthesis, Estuarine, Coastal and
1176 Shelf Science, 186, 1–10, https://doi.org/10.1016/j.ecss.2017.01.006, 2017b.

https://doi.org/10.5194/bg-2021-20
Preprint. Discussion started: 30 March 2021

1177 Mercado, J. M., Sobrino, C., Neale, P. J., Segovia, M., Reul, A., Amorim, A. L., Carrillo, P.,
1178 Claquin, P., Cabrerizo, M. J., León, P., Lorenzo, M. R., Medina-Sánchez, J. M.,
1179 Montecino, V., Napoleon, C., Prasil, O., Putzeys, S., Salles, S. and Yebra, L.: Effect of
1180 CO2, nutrients and light on coastal plankton. II. Metabolic rates, Aquatic Biology, 22,
1181 43–57, https://doi.org/10.3354/ab00606, 2014.
1182 Mills, M. M., Moore, C. M., Langlois, R., Milne, A., Achterberg, E., Nachtigall, K., Lochte, K.,
1183 Geider, R. J. and La, R. J.: Nitrogen and phosphorus co-limitation of bacterial
1184 productivity and growth in the oligotrophic subtropical North Atlantic, Limnology and
1185 Oceanography, 53(2), 824–834, https://doi.org/10.4319/lo.2008.53.2.0824, 2008.
1186 Mosseri, J., Quéguiner, B., Rimmelin, P., Leblond, N. and Guieu, C.: Silica fluxes in the
1187 northeast Atlantic frontal zone of Mode Water formation (38°–45°N, 16°–22°W) in
1188 2001–2002, Journal of Geophysical Research: Oceans, 110(C7),
1189 https://doi.org/10.1029/2004JC002615, 2005.
1190 Moulin, C. and Chiapello, I.: Impact of human-induced desertification on the intensification of
1191 Sahel dust emission and export over the last decades, Geophysical Research Letters,
1192 33(18), https://doi.org/10.1029/2006GL025923, 2006.
1193 Moutin, T. and Raimbault, P.: Primary production, carbon export and nutrients availability in
1194 western and eastern Mediterranean Sea in early summer 1996 (MINOS cruise), Journal of
1195 Marine Systems, 33–34, 273–288, https://doi.org/10.1016/S0924-7963(02)00062-3,
1196 2002.
1197 Moutin, T., Thingstad, T. F., Wambeke, F. V., Marie, D., Slawyk, G., Raimbault, P. and
1198 Claustre, H.: Does competition for nanomolar phosphate supply explain the
1199 predominance of the cyanobacterium Synechococcus?, Limnology and Oceanography,

47(5), 1562–1567, https://doi.org/10.4319/lo.2002.47.5.1562, 2002.

Müren, U., Berglund, J., Samuelsson, K. and Andersson, A.: Potential Effects of Elevated Sea-Water Temperature on Pelagic Food Webs, Hydrobiologia, 545(1), 153–166, https://doi.org/10.1007/s10750-005-2742-4, 2005.

Passow, U. and Carlson, C. A.: The biological pump in a high CO2 world, Marine Ecology Progress Series, 470, 249–271, 2012.

Polovina, J. J., Howell, E. A. and Abecassis, M.: Ocean's least productive waters are expanding, Geophysical Research Letters, 35(3), https://doi.org/10.1029/2007gl031745, 2008.

Pulido-Villena, E., Wagener, T. and Guieu, C.: Bacterial response to dust pulses in the western Mediterranean: Implications for carbon cycling in the oligotrophic ocean, Global Biogeochemical Cycles, 22(1), https://doi.org/10.1029/2007gb003091, 2008.

Pulido-Villena, E., Baudoux, A.-C., Obernosterer, I., Landa, M., Caparros, J., Catala, P., Georges, C., Harmand, J. and Guieu, C.: Microbial food web dynamics in response to a Saharan dust event: results from a mesocosm study in the oligotrophic Mediterranean Sea, Biogeosciences, 11(19), 5607–5619, 2014.

Regaudie-de-Gioux, A. and Duarte, C. M.: Temperature dependence of planktonic metabolism in the ocean, Global Biogeochemical Cycles, 26(1), https://doi.org/10.1029/2010GB003907, 2012.

Regaudie-de-Gioux, A., Vaquer-Sunyer, R. and Duarte, C. M.: Patterns in planktonic metabolism in the Mediterranean Sea, Biogeosciences, 6(12), 3081–3089, https://doi.org/10.5194/bg-6-3081-2009, 2009.

Ridame, C. and Guieu, C.: Saharan input of phosphate to the oligotrophic water of the open western Mediterranean Sea, Limnology and Oceanography, 47(3), 856–869, 2002.

https://doi.org/10.5194/bg-2021-20
Preprint. Discussion started: 30 March 2021

1223 Riebesell, U., Schulz, K. G., Bellerby, R. G. J., Botros, M., Fritsche, P., Meyerhofer, M., Neill,
1224 C., Nondal, G., Oschlies, A., Wohlers, J. and Zollner, E.: Enhanced biological carbon
1225 consumption in a high CO2 ocean, Nature, 450(7169), 545-U10, 2007.
1226 Smith, D. C. and Azam, F.: A simple, economical method for measuring bacterial protein
1227 synthesis rates in seawater using 3H-leucine, Marine Microbial Food Webs, 6(2), 107–
1228 114, 1992.
1229 Tanaka, T., Thingstad, T. F., Christaki, U., Colombet, J., Cornet-Barthaux, V., Courties, C.,
1230 Grattepanche, J.-D., Lagaria, A., Nedoma, J., Oriol, L., Psarra, S., Pujo-Pay, M. and
1231 Wambeke, F. V.: Lack of P-limitation of phytoplankton and heterotrophic prokaryotes in
1232 surface waters of three anticyclonic eddies in the stratified Mediterranean Sea,
1233 Biogeosciences, 8(2), 525–538, https://doi.org/10.5194/bg-8-525-2011, 2011.
1234 Ternon, E., Guieu, C., Loÿe-Pilot, M.-D., Leblond, N., Bosc, E., Gasser, B., Miquel, J.-C. and
1235 Martín, J.: The impact of Saharan dust on the particulate export in the water column of
1236 the North Western Mediterranean Sea, Biogeosciences, 7(3), 809–826,
1237 https://doi.org/10.5194/bg-7-809-2010, 2010.
1238 Thingstad, T. F., Krom, M. D., Mantoura, R. F. C., Flaten, G. a. F., Groom, S., Herut, B., Kress,
1239 N., Law, C. S., Pasternak, A., Pitta, P., Psarra, S., Rassoulzadegan, F., Tanaka, T.,
1240 Tselepides, A., Wassmann, P., Woodward, E. M. S., Riser, C. W., Zodiatis, G. and
1241 Zohary, T.: Nature of Phosphorus Limitation in the Ultraoligotrophic Eastern
1242 Mediterranean, Science, 309(5737), 1068–1071, https://doi.org/10.1126/science.1112632,
1243 2005.
1244 Van Wambeke, F., Taillandier, V., Deboeufs, K., Pulido-Villena, E., Dinasquet, J., Engel, A.,
1245 Marañón, E., Ridame, C. and Guieu, C.: Influence of atmospheric deposition on

https://doi.org/10.5194/bg-2021-20
Preprint. Discussion started: 30 March 2021

biogeochemical cycles in an oligotrophic ocean system, Biogeosciences Discussions, 1–51, https://doi.org/10.5194/bg-2020-411, 2020a.

Van Wambeke, F., Pulido, E., Dinasquet, J., Djaoudi, K., Engel, A., Garel, M., Guasco, S., Nunige, S., Taillandier, V., Zäncker, B. and Tamburini, C.: Spatial patterns of biphasic ectoenzymatic kinetics related to biogeochemical properties in the Mediterranean Sea, Biogeosciences Discussions, 1–38, https://doi.org/10.5194/bg-2020-253, 2020b.

Wang, Q., Lyu, Z., Omar, S., Cornell, S., Yang, Z. and Montagnes, D. J. S.: Predicting temperature impacts on aquatic productivity: Questioning the metabolic theory of ecology's "canonical" activation energies, Limnology and Oceanography, 64(3), 1172–1185, https://doi.org/10.1002/lno.11105, 2019.

Zobell, C. E. and Anderson, D. Q.: Observations on the multiplication of bacteria in different volumes of stored sea water and the influence of oxygen tension and solid surfaces, The Biological Bulletin, 71(2), 324–342, https://doi.org/10.2307/1537438, 1936.

Tables

Table 1. Initial chemical and biological stocks as measured while filling the tanks (initial conditions in pumped surface water; sampling time: t-12h). NO_x: nitrate + nitrite, DIP: dissolved inorganic phosphorus, $Si(OH)_4$: silicate, POC: particulate organic carbon, DOC: dissolved organic carbon, TEP: transparent exopolymer particles, TChl*a*: total chlorophyll *a*. Values shown for ^{14}C incorporation rates, percentages of extracellular release (%PER) as well as for net community production (NCP), community respiration (CR) and gross primary production (GPP) were estimated from samples taken at t0 in the control tanks. For heterotrophic bacterial production (BP), rates were estimated from seawater sampled at t-12h.

	Sampling station	TYR	ION	FAST
	Coordinates (decimal)	39.34 N, 12.60 E	35.49 N, 19.78 E	37.95 N, 2.90 N
	Bottom depth (m)	3395	3054	2775
	Day and time of pumping (local time)	17/05/2017 17:00	25/05/2017 17:00	02/06/2017 21:00
	Temperature (°C)	20.6	21.2	21.5
	Salinity	37.96	39.02	37.07
Stocks	NO_x (nmol L^{-1})	14.0	18.0	59.0
	DIP (nmol L^{-1})	17.1	6.5	12.9
	$Si(OH)_4$ (µmol L^{-1})	1.0	0.96	0.64

	POC (µmol L^{-1})	12.9	8.5	6.0
	DOC (µmol L^{-1})	72.2	70.2	69.6
	TEP (x 10^6 L^{-1})	6.8	3.8	3.7
	TChl*a* (µg L^{-1})	0.063	0.066	0.072
	Heterotrophic prokaryotes abundance (x 10^5 cell mL^{-1})	4.79	2.14	6.15
Processes	^{14}C-based total particulate production (µg C L^{-1} h^{-1})	0.08 ± 0.03	0.14 ± 0.04	0.15 ± 0.04
	^{14}C-based > 2 µm particulate production (µg C L^{-1} h^{-1})	0.07 ± 0.02	0.11 ± 0.02	0.11 ± 0.02
	^{14}C-based < 2 µm particulate production (µg C L^{-1} h^{-1})	0.01 ± 0.01	0.04 ± 0.02	0.05 ± 0.01
	%PER	60 ± 20	45 ± 3	32 ± 23
	NCP (µmol O_2 L^{-1} d^{-1})	-1.9 ± 0.3	-0.2 ± 0.2	-0.8 ± 0.9
	CR (µmol O_2 L^{-1} d^{-1})	-2.6 ± 0.1	-1.2 ± 0.5	-1.9 ± 1.6
	GPP (µmol O_2 L^{-1} d^{-1})	0.7 ± 0.4	1.1 ± 0.3	1.1 ± 0.7
	BP (ng C L^{-1} h^{-1})	11.6	15.2	34.6

1266

https://doi.org/10.5194/bg-2021-20
Preprint. Discussion started: 30 March 2021

1267 Table 2. Heterotrophic bacterial production (BP) growth rates (μ_{BP} in h^{-1}) estimated from the
1268 exponential phase of BP growth, observable from at least four sampling points, between t0 and
1269 t12h, during the three experiments (TYR, ION and FAST) in the six tanks (controls: C1, C2; dust
1270 addition under present conditions of temperature and pH: D1, D2; dust addition under future
1271 conditions of temperature and pH: G1 and G2). Values ± SE are shown.

	μ_{BP}		
	TYR	ION	FAST
C1	0.076 ± 0.025	0.042 ± 0.007	0.020 ± 0.003
C2	0.066 ± 0.018	0.041 ± 0.005	0.026 ± 0.004
D1	0.117 ± 0.008	0.095 ± 0.020	0.089 ± 0.014
D2	0.194 ± 0.020	0.145 ± 0.007	0.090 ± 0.007
G1	0.164 ± 0.020	0.126 ± 0.011	0.124 ± 0.005
G2	0.150 ± 0.003	0.137 ± 0.033	0.163 ± 0.014

1272

https://doi.org/10.5194/bg-2021-20
Preprint. Discussion started: 30 March 2021

1273 Table 3. Estimated bacterial growth efficiency (BGE in %) during the course of the three
1274 experiments (TYR, ION and FAST) in the six tanks (controls: C1, C2; dust addition under
1275 present conditions of temperature and pH: D1, D2; dust addition under future conditions of
1276 temperature and pH: G1 and G2). BGE was calculated based on integrated heterotrophic
1277 bacterial production (BP) and community respiration (CR) rates by applying a bacterial
1278 respiration to CR ratio of 0.7 and a respiratory quotient of 0.8 (see Material and Methods).

	Bacterial growth efficiency (BGE)		
	TYR	ION	FAST
C1	11.1	9.8	15.4
C2	11.7	14.5	22.0
D1	31.8	21.0	17.3
D2	32.3	30.6	19.9
G1	39.3	35.2	37.6
G2	32.5	34.8	38.1

1279

1280

https://doi.org/10.5194/bg-2021-20
Preprint. Discussion started: 30 March 2021

1281 # Figure caption

1282 Fig. 1. Map showing the sampling stations in the Mediterranean Sea along the transect performed
1283 onboard the R/V "Pourquoi Pas ?" during the PEACETIME cruise.

1284 Fig. 2. Dissolved organic carbon (DOC) concentrations and ratio between total hydrolysable
1285 amino acids (TAA) and DOC concentrations measured in the six tanks (controls: C1, C2; dust
1286 addition under present conditions of temperature and pH: D1, D2; dust addition under future
1287 conditions of temperature and pH: G1 and G2) during the three experiments (TYR, ION and
1288 FAST). The dashed vertical line indicates the time of seeding (after t0).

1289 Fig. 3. Particulate organic carbon (POC) concentrations and transparent exopolymer particle
1290 carbon content (TEP-C) measured in the six tanks (controls: C1, C2; dust addition under present
1291 conditions of temperature and pH: D1, D2; dust addition under future conditions of temperature
1292 and pH: G1 and G2) during the three experiments (TYR, ION and FAST). The dashed vertical
1293 line indicates the time of seeding (after t0).

1294 Fig. 4. ^{14}C-based production rates (< 2 µm and > 2 µm size fractions, total particulate) estimated
1295 from 8 h incubations on samples taken in the six tanks (controls: C1, C2; dust addition under
1296 present conditions of temperature and pH: D1, D2; dust addition under future conditions of
1297 temperature and pH: G1 and G2) during the three experiments (TYR, ION and FAST). The
1298 percentage of extracellular release (%PER) is also shown.

1299 Fig. 5. Incorporation of ^{13}C into particulate organic carbon ($\delta^{13}C$-POC) in the six tanks (controls:
1300 C1, C2; dust addition under present conditions of temperature and pH: D1, D2; dust addition

https://doi.org/10.5194/bg-2021-20
Preprint. Discussion started: 30 March 2021

1301 under future conditions of temperature and pH: G1 and G2) during the three experiments (TYR,
1302 ION and FAST). The dashed vertical line indicates the time of seeding (after t0).

1303 Fig. 6. Net community production (NCP), community respiration (CR) and gross primary
1304 production (GPP) rates estimated using the oxygen light-dark method (24 h incubations) on
1305 samples taken in the six tanks (C1, C2, D1, D2, G1 and G2) during the three experiments (TYR,
1306 ION and FAST).

1307 Fig. 7. Heterotrophic bacterial production rates (BP) and cell-specific maximum hydrolysis
1308 velocity (Vm) of the alkaline phosphatase (both over 1-2 h incubations) on samples taken in the
1309 six tanks (C1, C2, D1, D2, G1 and G2) during the three experiments (TYR, ION and FAST).

1310 Fig. 8. Total mass and organic matter fluxes measured in the sediment traps at the end of the
1311 three experiments (TYR, ION and FAST) in the six tanks (C1, C2, D1, D2, G1 and G2).

1312 Fig. 9. Relative difference (%) between integrated rates measured in tanks D (D1, D2; dust
1313 addition under present conditions of temperature and pH) and G (G1, G2; dust addition under
1314 future conditions of temperature and pH) as compared to the controls (C1, C2) during the three
1315 experiments (TYR, ION and FAST). Vertical boxes represent the range observed between the
1316 two replicates per treatment.

https://doi.org/10.5194/bg-2021-20
Preprint. Discussion started: 30 March 2021

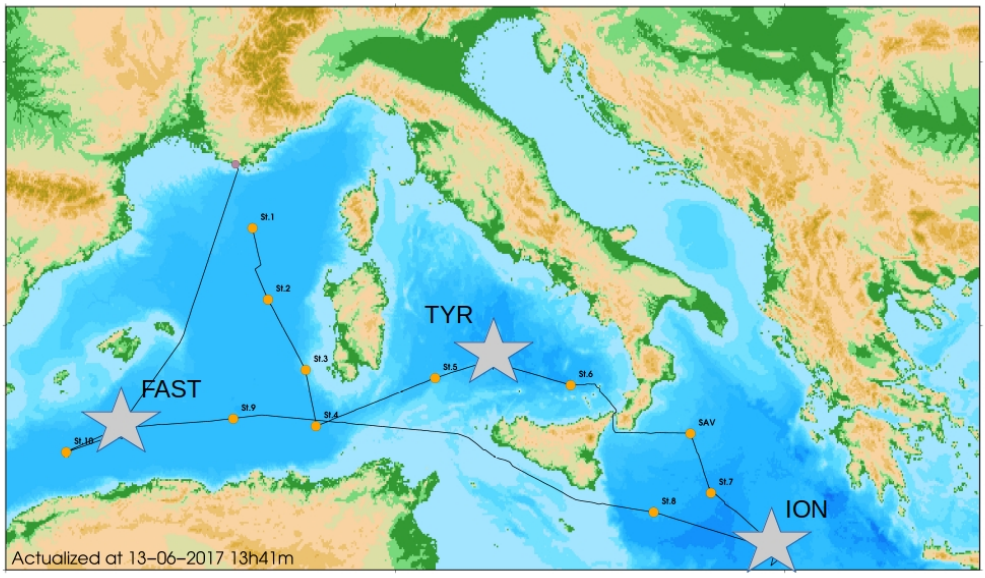

1317

1318 Fig. 1

https://doi.org/10.5194/bg-2021-20
Preprint. Discussion started: 30 March 2021

Biogeosciences
Discussions
Open Access
EGU

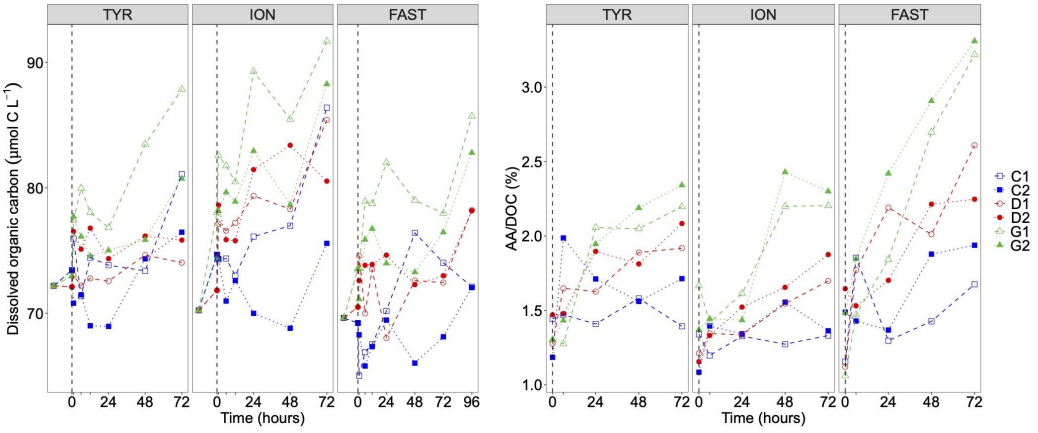

1319

1320 Fig. 2

https://doi.org/10.5194/bg-2021-20
Preprint. Discussion started: 30 March 2021

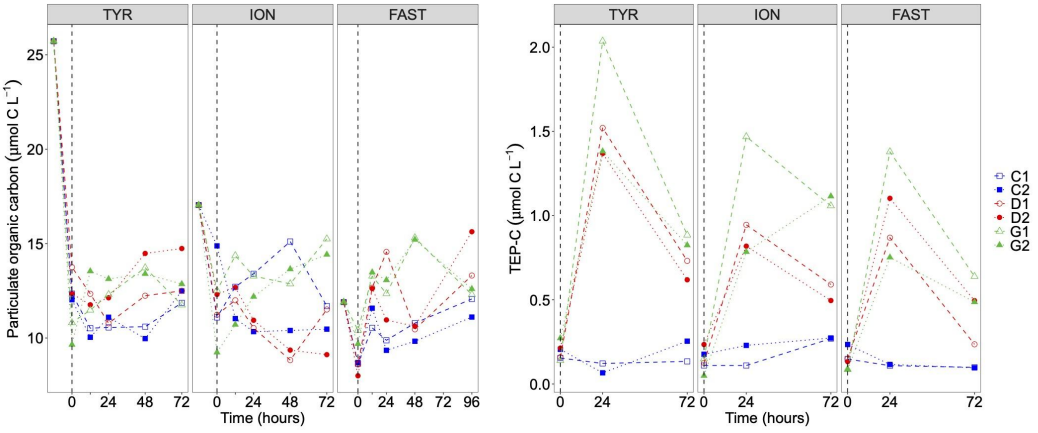

1321

1322 Fig. 3

https://doi.org/10.5194/bg-2021-20
Preprint. Discussion started: 30 March 2021

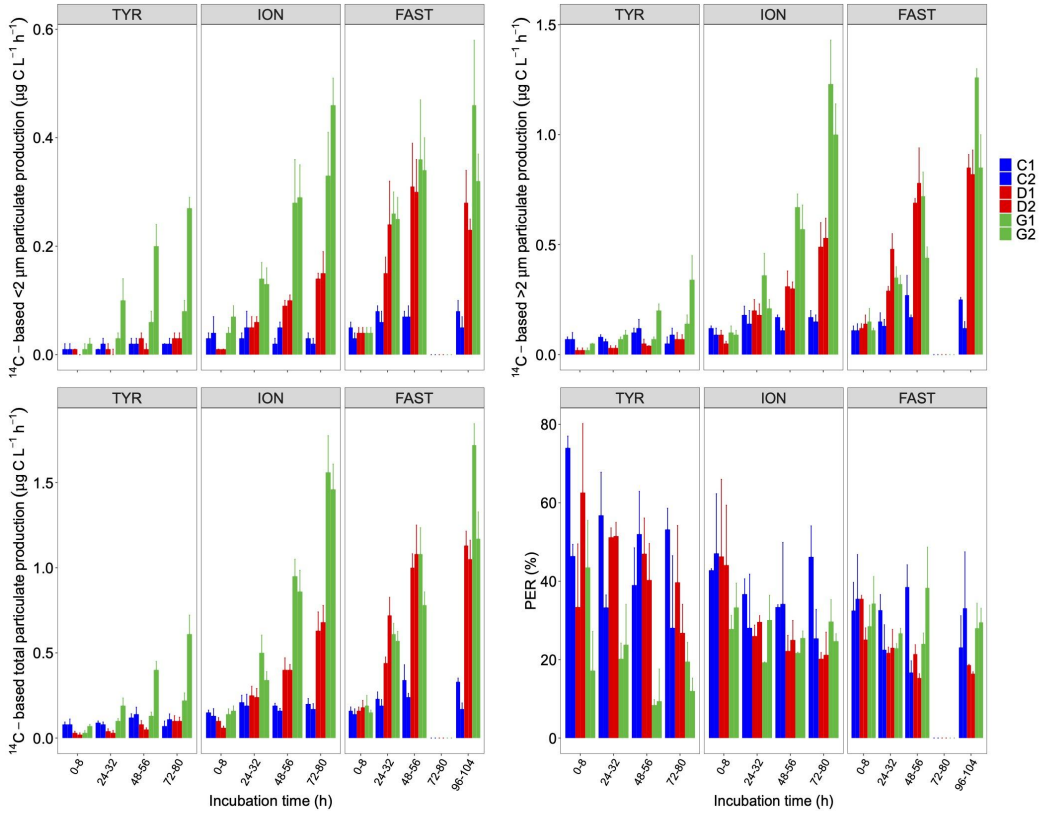

1323

1324 Fig. 4

https://doi.org/10.5194/bg-2021-20
Preprint. Discussion started: 30 March 2021

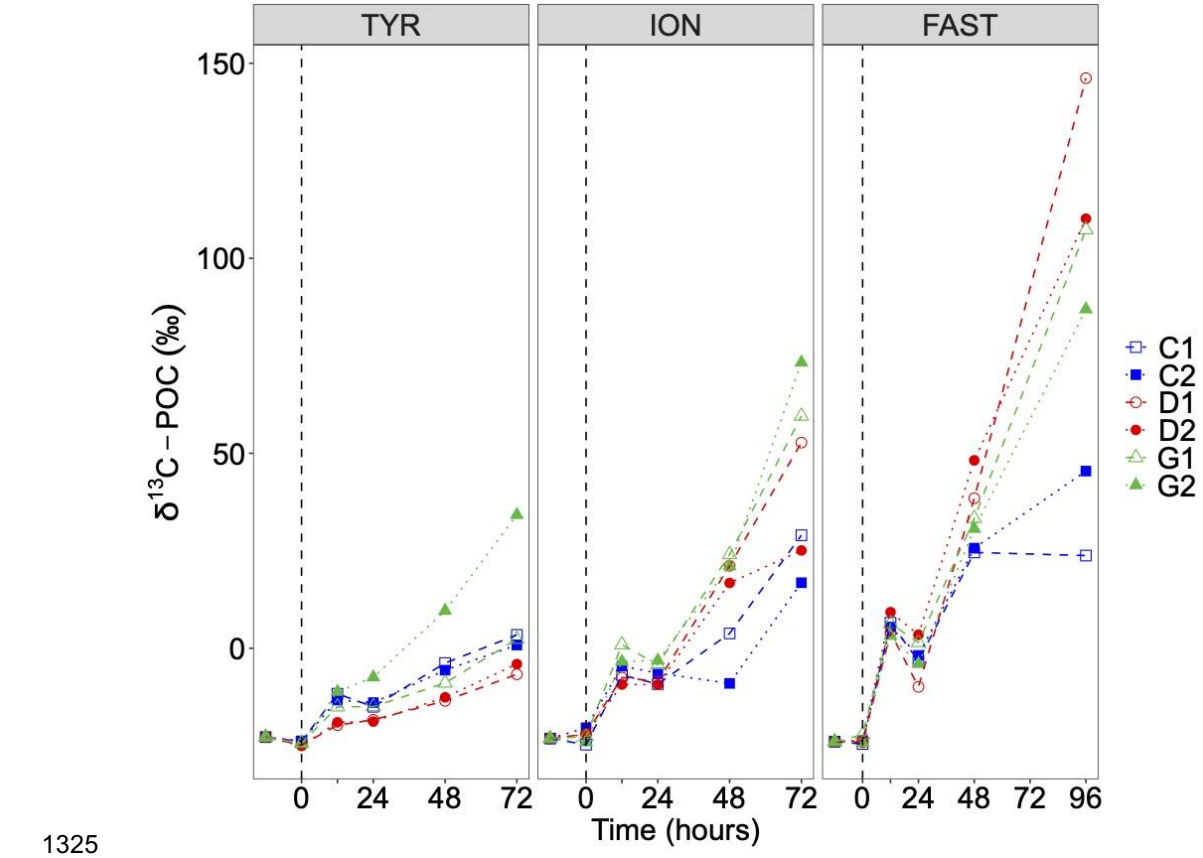

1325

1326 Fig. 5

https://doi.org/10.5194/bg-2021-20
Preprint. Discussion started: 30 March 2021

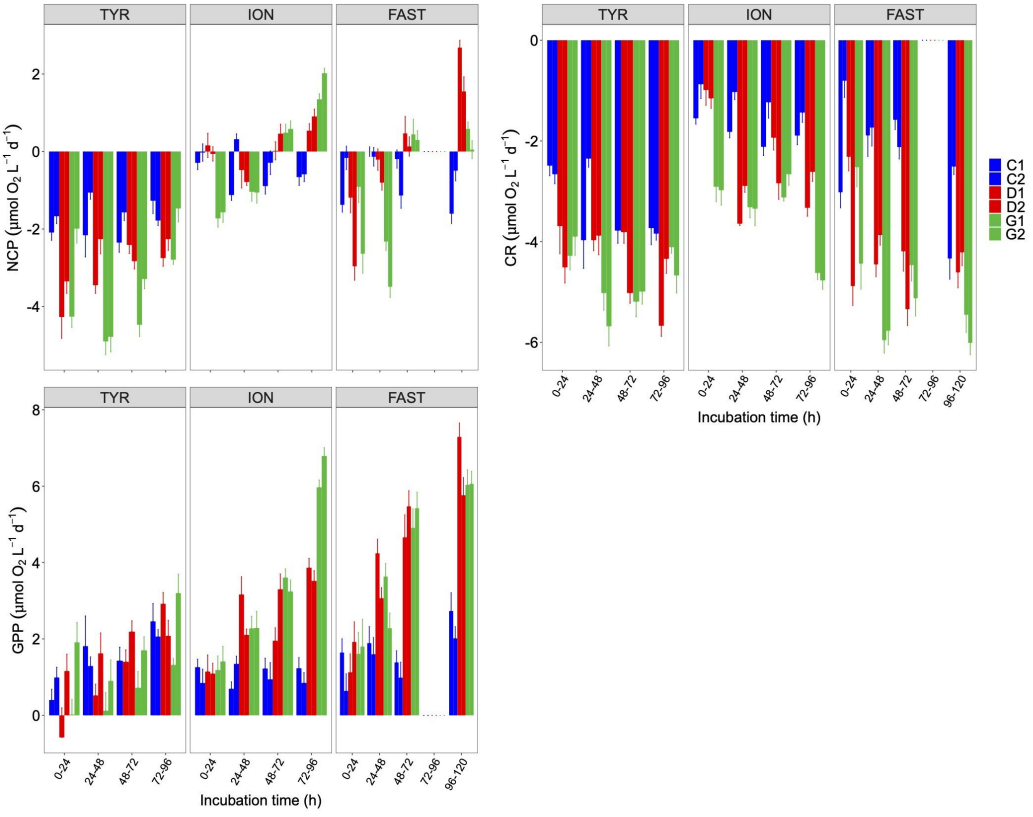

1327

1328 Fig. 6

https://doi.org/10.5194/bg-2021-20
Preprint. Discussion started: 30 March 2021

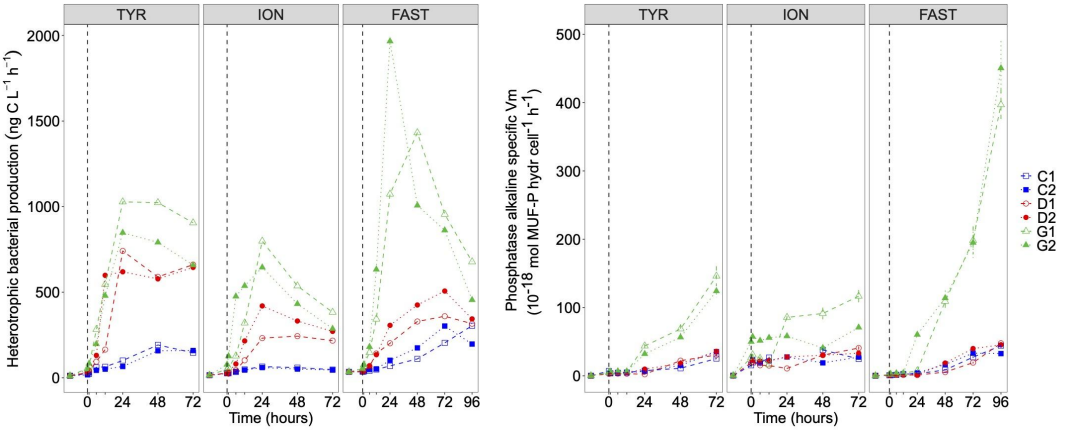

1329

1330 Fig. 7

https://doi.org/10.5194/bg-2021-20
Preprint. Discussion started: 30 March 2021

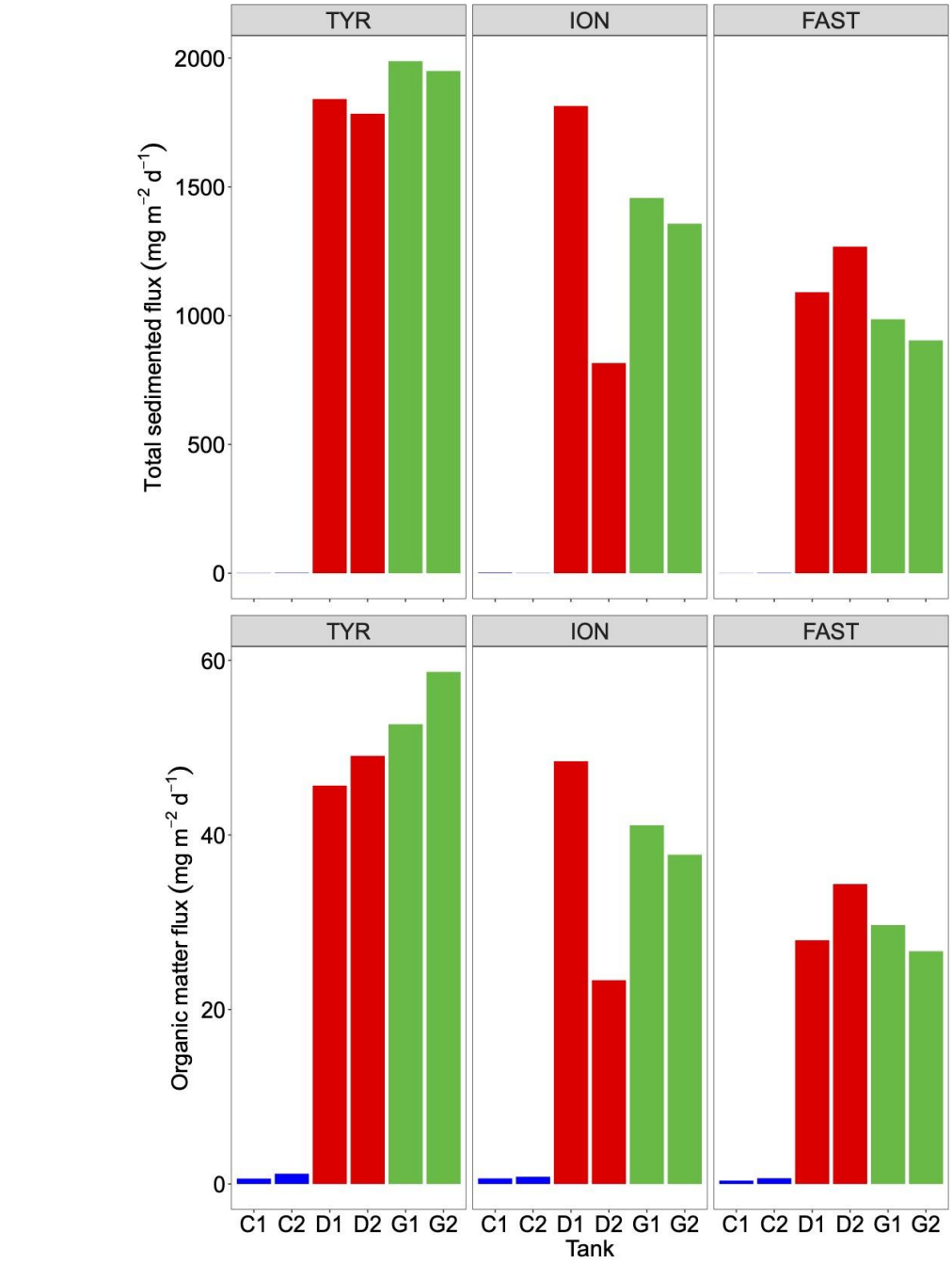

1331

1332 Fig. 8

https://doi.org/10.5194/bg-2021-20
Preprint. Discussion started: 30 March 2021

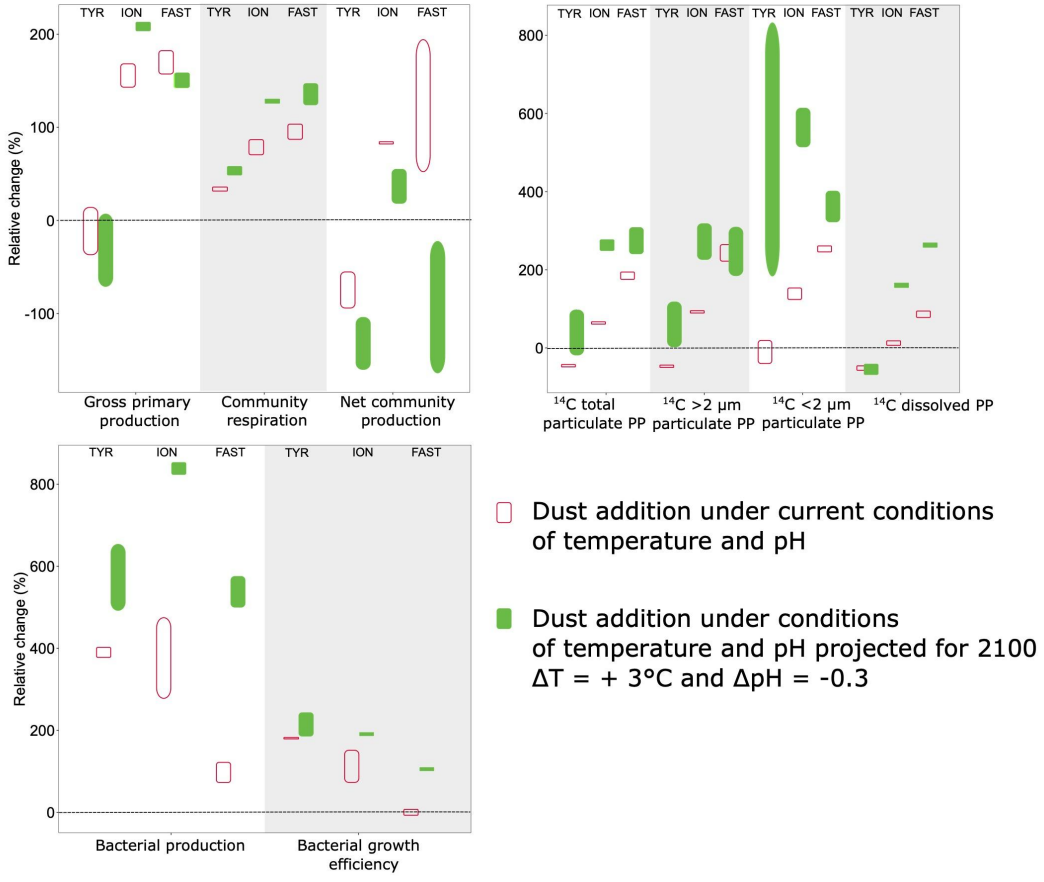

1333

1334 Fig. 9